LBL-23305
Preprint c.2

# Lawrence Berkeley Laboratory
UNIVERSITY OF CALIFORNIA

## Engineering Division

RECEIVED
LAWRENCE
BERKELEY LABORATORY

NOV 20 1987

LIBRARY AND
DOCUMENTS SECTION

Submitted to Physical Review B

# Trigonal Hydrogen-Related Acceptor Complexes in Germanium

J.M. Kahn, R.E. McMurray, Jr.,
E.E. Haller and L.M. Falicov

May 1987

TWO-WEEK LOAN COPY
This is a Library Circulating Copy
which may be borrowed for two weeks.

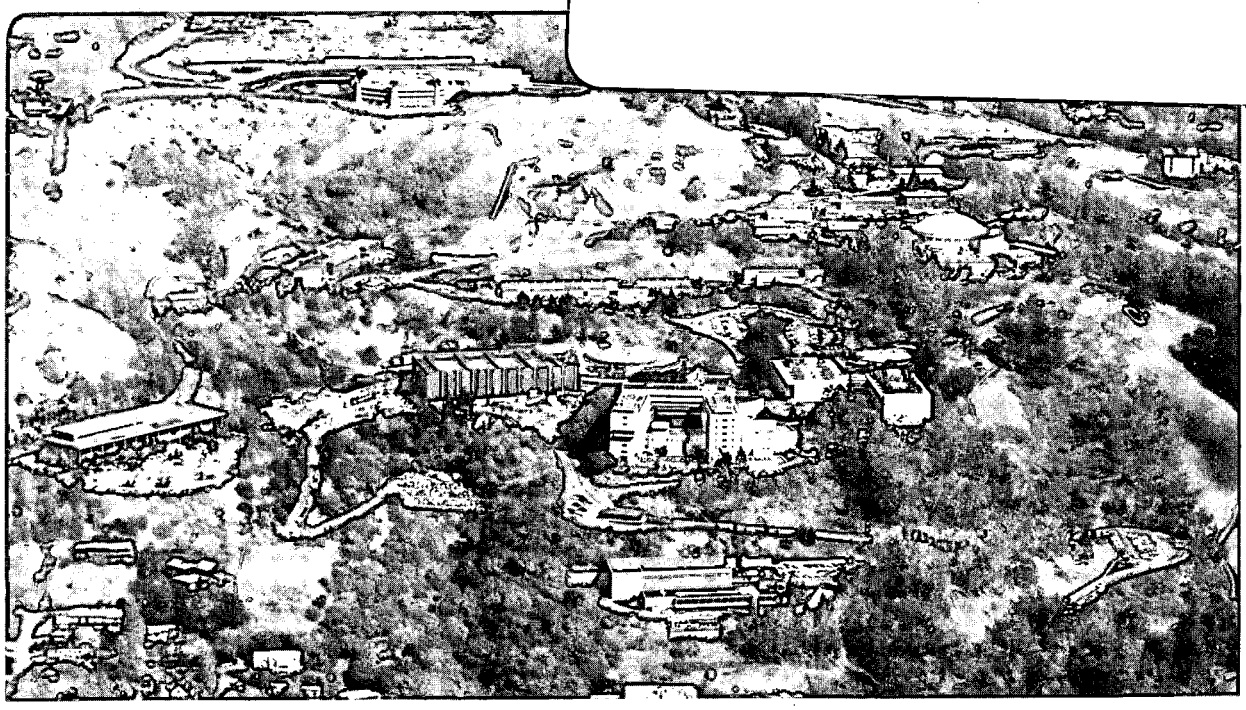

LBL-23305
c.2

Prepared for the U.S. Department of Energy under Contract DE-AC03-76SF00098

## DISCLAIMER

This document was prepared as an account of work sponsored by the United States Government. While this document is believed to contain correct information, neither the United States Government nor any agency thereof, nor the Regents of the University of California, nor any of their employees, makes any warranty, express or implied, or assumes any legal responsibility for the accuracy, completeness, or usefulness of any information, apparatus, product, or process disclosed, or represents that its use would not infringe privately owned rights. Reference herein to any specific commercial product, process, or service by its trade name, trademark, manufacturer, or otherwise, does not necessarily constitute or imply its endorsement, recommendation, or favoring by the United States Government or any agency thereof, or the Regents of the University of California. The views and opinions of authors expressed herein do not necessarily state or reflect those of the United States Government or any agency thereof or the Regents of the University of California.

# Trigonal Hydrogen-Related Acceptor Complexes in Germanium

J. M. Kahn,* Robert E. McMurray, Jr., E. E. Haller and L. M. Falicov

University of California and Lawrence Berkeley Laboratory

Berkeley, California 94720

In germanium, an interstitial hydrogen atom may bind at a substitutional atom of carbon, silicon, beryllium or zinc to form a shallow, monovalent acceptor complex. Photothermal ionization spectroscopy under uniaxial stress reveals that the complexes A(H,C), A(H,Si), A(Be,H) and A(Zn,H) have trigonal ($\overline{C}_{3v}$) symmetry. Each has two (1s)-like acceptor levels which shift, but do not split, under stress. In the fourfold basis for a $\Gamma_8(\overline{T}_d)$ level, simultaneous diagonalization of the perturbations of applied stress, and of a trigonal lowering of symmetry, yields theoretical piezospectroscopic behavior in quantitative agreement with all available experimental data. This procedure has been extended to predict the stress-induced shifts of (1s)-like shallow acceptor levels associated with tetragonal ($\overline{D}_{2d}$) and rhombic I ($\overline{C}_{2v}$) complexes in germanium, should these ever be observed experimentally. The four trigonal complexes in germanium are to be contrasted with A(Be,H) in silicon, in which the rapid tunneling of hydrogen leads to recovery of tetrahedral symmetry and a much more complicated energy level structure.

## I. INTRODUCTION

The hydrogen-carbon and hydrogen-silicon shallow acceptor complexes[1] in germanium, designated A(H,C) and A(H,Si), were studied previously by means of photothermal ionization spectroscopy[2] (PTIS) in conjunction with uniaxial stress. They were modeled as dynamic centers in which the rapid tunneling of hydrogen nuclei gives rise to a recovery of tetrahedral symmetry and a manifold of five (1s)-like acceptor levels with unconventional behavior under uniaxial stress. We report new uniaxial-stress PTIS measurements which demonstrate that both A(H,C) and A(H,Si) have trigonal symmetry and exhibit no evidence of tunneling hydrogen. The beryllium-hydrogen and zinc-hydrogen shallow acceptor complexes,[3] A(Be,H) and A(Zn,H), are known to have trigonal symmetry. We present a simple theoretical model which quantitatively explains the stress-induced shifts of the acceptor levels of A(H,C), A(H,Si), A(Be,H) and A(Zn,H). The model is also extended to predict the piezospectroscopic behavior of tetragonal and rhombic I shallow acceptor complexes.

We begin with a brief discussion of hydrogen-related impurity complexes in semiconductors. Many studies have demonstrated the passivation by atomic hydrogen of deep-level defects in silicon,[4] germanium[5] and other semiconductors. It has also been shown that hydrogen can neutralize the electrical activity of shallow acceptors such as boron in silicon,[6-8] and of shallow donors such as phosphorus in silicon.[9] There is no general agreement on models which explain the passivation processes on a microscopic scale.

A special group of hydrogen-related defects are those which have associated shallow or semi-deep donor or acceptor levels. These electrically active centers can be studied with high sensitivity and high energy resolution using optical spectroscopy, allowing one to obtain detailed information on the multiplicity and symmetry of the impurity states. Growth of high-purity

germanium[10,11] crystals from a silica ($SiO_2$) crucible under hydrogen is known to result in the incorporation of ~$10^{15}$ $cm^{-3}$ atoms of hydrogen,[12] ~$10^{15}$ $cm^{-3}$ atoms of silicon, and 5-10 x $10^{13}$ $cm^{-3}$ atoms of oxygen, all electrically inactive as isolated species. Rapid quenching of such samples from ~450°C creates[13] a shallow acceptor; this acceptor converts quickly at room temperature into a shallow donor which is stable to somewhat higher temperatures. Substitution of deuterium results in isotope shifts[14] of electronic transitions of the donor (51±3 μeV) and of the acceptor (21±3 μeV), proving that each center contains hydrogen. Correlation with precise measurements of the oxygen and silicon concentrations allowed the assignment of the donor to a hydrogen-oxygen complex designated D(H,O),[15] and of the acceptor to a hydrogen-silicon complex A(H,Si).[1] PTIS measurements showed that the spectrum of D(H,O) exhibits an unusual behavior under uniaxial stress. This center has been modeled in terms of a rapidly tunneling, substitutional (OH) complex.[15]

A shallow acceptor complex is found always and only in high-purity germanium crystals grown from a graphite crucible under hydrogen, and has been designated[1] A(H,C). It has been argued that both A(H,Si) and A(H,C) are formed when an interstitial hydrogen atom becomes trapped in the strain field near one of the substitutional, isovalent impurities, which have covalent radii smaller than the host (i.e., substitutional tin does not bind a hydrogen atom). PTIS studies showed that associated with each complex is a pair of (1s)-like acceptor levels (see Table I), separated by a splitting of the order of 1 meV, and with average energy near the (1s) ground state, calculated in effective-mass theory.[18] Only the (1s)-like ground state level is occupied at zero temperature; the shallower (1s)-like level is populated according to Boltzmann statistics at finite temperature. No splitting of the (1s)-like levels of

A(H,Si) and A(H,C) could be detected under applied uniaxial stress, and it was proposed that the zero-point motion of the hydrogen atom involves rapid tunneling among four <111> directions.[1] As a consequence, each of these centers would have full tetrahedral symmetry despite its inherently asymmetric structure, and would have a manifold of five (1s)-like acceptor levels. The two deepest levels were assumed to be Kramers doublets with $\Gamma_6$ and $\Gamma_7(\overline{T}_d)$ symmetry,[19] so that they would not split under stress. The model predicted the existence of three $\Gamma_8(\overline{T}_d)$ levels which would split understress, but these have never been observed experimentally.

Muro and Sievers recently showed that in silicon, a single atom of hydrogen or deuterium transforms the divalent acceptor beryllium into the monovalent acceptor complexes A(Be,H) and A(Be,D) respectively.[20] The light nuclei appear to tunnel rapidly, producing a multiplicity of (1s)-like acceptor levels consistent with the model for acceptors with tunneling hydrogen,[1] and splitting the p-like bound-excited-state levels. A more complicated set of hydrogen-related, dynamic acceptor complexes are A(Cu,Y,Z) in germanium, with Y,Z = H,D,T, in which the nuclear motion exhibits an abrupt transition from tunneling to libration, induced by an increase in hydrogen isotopic mass.[21]

In germanium grown under a hydrogen ambient and intentionally doped with the divalent acceptors beryllium and zinc, PTIS revealed the shallow, monovalent acceptor complexes A(Be,H) and A(Zn,H).[3] Uniaxial stress showed that each has trigonal symmetry; the reduction from tetrahedral symmetry splits the $\Gamma_8(\overline{T}_d)$ (1s)-like level into $\Lambda_4$ and $\Lambda_{5,6}(\overline{C}_{3v})$ levels. Both levels have been observed for A(Be,H) (see Table I); for A(Zn,H), the splitting is apparently too large to allow population of the second level below a temperature at which complete ionization occurs.

The remainder of this paper is organized as follows. In Section II, we describe the experimental procedures employed. Section III presents experimental results which emphasize piezospectroscopic studies of A(H,C), A(H,Si), A(Be,H) and A(Zn,H). In Section IV, we develop a theory of the piezospectroscopy of shallow acceptors which have trigonal, tetragonal and rhombic I symmetries, and describe its application to hydrogen-related trigonal centers. We conclude this paper with the discussion of Section V.

## II. EXPERIMENTAL PROCEDURE

For the data on A(Be,H) and A(Zn,H) which are included here, details of sample preparation and measurement have been described elsewhere.[3] For the study of A(H,Si) and A(H,C), high-purity germanium material was selected as in previous work.[1] Samples for unstressed measurements were 2 x 6.5 x 6.5 $mm^3$ in size. For stressed measurements, 2 x 2 x 6.5 $mm^3$ samples were oriented with their long dimension parallel to the desired crystallographic axis, making reference to the boule growth axis and known crystal habit (accurate to approximately ±2°). Samples were sawed, lapped with 1900 grit, etched for 2 min in a 3:1 $HNO_3$:HF mixture and rinsed in electronic-grade methanol. Electrical contacts were formed by implantation of 25 keV B+ ions to a dose of 2 x $10^{14}$ $cm^{-2}$, and were electrically active as implanted. Samples for unstressed measurements were contacted on opposing 2 x 6.5 $mm^2$ faces; those for stress were contacted with two 2 x 2 $mm^2$ squares, placed 2 mm apart in the center of one 2 x 6.5 $mm^2$ face. All samples were annealed at 450°C for 15 min under an inert atmosphere, and then quenched into liquid nitrogen. Samples containing A(H,Si) were stored in liquid nitrogen prior to measurement.

The low concentrations ($10^{10}$-$10^{11}$ $cm^{-3}$) of the acceptors under study dictate use of the sensitive PTIS technique.[2] With the impurity center in a

(1s)-like state, absorption of a photon at a discrete transition energy is followed by thermal ionization from the bound excited state, detected as an increase of the sample conductivity. During measurement, samples were held at a controlled temperature between 4.2 and 10 K, and were shielded from all radiation above 100 $cm^{-1}$ (250 $cm^{-1}$ in some cases) using Yoshinaga-type filters[22] and black polyethylene. All spectra were recorded using a custom-built Fourier transform spectrometer[23] with attainable energy resolution of 0.025 $cm^{-1}$ (~3 μeV); spectra reported here were recorded with resolution in the range 0.045-0.077 $cm^{-1}$ (6-10 μeV), and were fully resolved in all cases. For uniaxial stress measurements, samples were placed with thin cardboard pads against the ends in a spring-and-lever apparatus.[24] By employing samples of greater length-to-width ratio and spectroscopically probing only the central region in which the stress is uniform, we obtain better resolution of stress-split components as compared to a previous study.[1] Analysis of spectra recorded with unpolarized radiation is sufficient here.

In the absence of stress, we label transitions in the usual notation.[25] We label stress-split transitions (and their energies) using the same notation, adding subscripts in order of increasing energy. Because the apparatus could not yield accurately calibrated small values of stress, the stress magnitude was measured through the following procedure. We equated the observed splitting of the aluminum D transition ($1\Gamma_8^+ \rightarrow 2\Gamma_8^-$) to what is expected for the gallium acceptor, using theoretical expressions incorporating the experimentally measured impurity deformation potentials[26] and elastic compliance[27] constants. (See Section IV.A for a detailed discussion of the theory and of the values used.) For [111] stress, we used the expression:

$$D_2 - D_1 = \Delta_i^{Ga}, \tag{1}$$

with i = [111]; for [100] and [110], we employed:

$$D_3 - D_2 = \Delta_i^{Ga} - \Delta_i^{D}, \tag{2}$$

with i = [100],[110]. Here $\Delta_i^{Ga}$ is the splitting of the gallium $1\Gamma_8^+$ level, given by the difference of the the shifts of the two stress-induced sublevels (see Table III); $\Delta_i^{D}$ is the corresponding splitting for the $2\Gamma_8^-$ level. Stress values thus calculated are subject to an overall scaling uncertainty of ±2%, ±14% and ±7% for [111], [100] and [110], due to uncertainties in the experimentally measured values of the deformation potential constants.[26] Additional errors are introduced because we use the deformation potentials of the gallium $1\Gamma_8^+$ level ($b'_{Ga}$ = -1.33±0.03 eV, $d'_{Ga}$ = -2.91±0.06 eV) to describe the splitting of aluminum, since no published values could be found for the latter acceptor. For the acceptor indium,[28] $b'_{In}$ = -1.4±0.2 eV and $d'_{In}$ = -2.9±0.4 eV, equal within experimental error to the corresponding values for gallium. Aluminum has a binding energy[18,25] of 11.15 meV, much closer to the 11.32 meV value for of gallium than is the 11.99 meV value for indium. Since differences in binding energy reflect differences in the (1s)-like envelope functions, we expect that $b'_{Al}$ and $d'_{Al}$ are close to the respective values for gallium; it seems likely that any differences are of the order of less than 5%.

## III. EXPERIMENTAL RESULTS

### A. High-resolution studies of A(H,C) and A(H,Si)

Figure 1 shows the PTI spectrum of a sample containing boron, aluminum and the deuterium-carbon acceptor complex,[1] A(D,C). Compared to previous high-resolution studies[25] of shallow acceptors in germanium, there is additional structure in the region labeled "I", so that we resolve as many as 19 transitions from a single (1s)-like level. The narrowest lines in this spectrum [e.g., the B transition of $A(D,C)_2$] have full widths at half maximum (FWHM) of 0.09 $cm^{-1}$ (11 μeV). The D and C transitions from the excited level $A(D,C)_1$ are considerably broader [FWHM of 0.25 $cm^{-1}$ (31 μeV)] than the corresponding transitions from the ground-state level $A(D,C)_2$ [FWHM of 0.11 $cm^{-1}$ (14 μeV)]. For transitions from the level $A(D,C)_2$, the spacing among the strongest transitions (D, C, B) is identical to that in the spectra of aluminum and gallium, within 5 μeV. We have also performed PTIS studies of A(H,C) (obtained in the usual way[1]), and of A(T,C), found in samples taken from crystals grown under vacuum out of graphite crucibles, which were subsequently exposed to plasmas of nearly pure tritium.[23] We observed no isotope shifts of transitions from the (1s)-like ground state levels, to a limit of 5 μeV.

We have also recorded high-resolution PTI spectra of the hydrogen-silicon acceptor complex, A(H,Si). Transitions from the excited (1s)-like level $A(H,Si)_1$ are noticeably broader [FWHM of 0.39 $cm^{-1}$ (48 μeV)] than the corresponding transitions from the ground-state level $A(H,Si)_2$ [FWHM of 0.14 $cm^{-1}$ (17 μeV)]. Among the strongest transitions (D, C, B) from the level $A(H,Si)_2$, the spacing is identical to that found in the spectra of boron and aluminum, within 5 μeV.

B. Piezospectroscopic studies of A(H,C) and A(H,Si)

Figure 2 shows the PTI spectra of the D and C transitions of aluminum, and the D transition of $A(D,C)_2$, under uniaxial compression along [111], [100] and [110]. These spectra were recorded under a set of conditions[29] which precluded observation of transitions from the excited (1s)-like level, $A(D,C)_1$. The oscillatory structure apparent in Fig. 2(a) is the artifact of coherent multiple internal reflections between opposing plane-parallel faces of the sample. Splitting of the aluminum D line follows the well-known behavior of a $\Gamma_8 \rightarrow \Gamma_8$ transition (see Section IV.A for a detailed discussion). In principle, both the ground-state and final-state levels split into two levels, allowing observation of four D lines with unpolarized radiation. Under [111] stress, the splitting of the final state of the D transition is unobservably small, so that only two D lines are observed.

Examination of Fig. 2 shows that the behavior of the aluminum C line is more complex than that of the D line: the former splits into three lines under [111] stress, six under [100] stress, and five under [110] stress. This supports the theoretical prediction that the final state of the C transition consists of nearly degenerate $3\Gamma_8^-$ and $1\Gamma_7^-$ levels.[18] Although this coincidence of levels is apparently accidental, it must be exact within about 6 μeV, to explain the observation that the C line is not wider than the D line (see Fig. 1). Detailed measurements of the gallium C line are in progress elsewhere,[30] and have yielded at least as many stress-induced components as we report here.

It is apparent in Fig. 2(a) that under [111] stress, the D line of $A(D,C)_2$ evolves into two lines $D_1$ and $D_2$; $D_2$ is evident as a shoulder to the right of $D_1$ in the spectrum recorded at 0.039 kbar. We note that $D_1$ has about three times the intensity of $D_2$. In the [100] spectra of Fig. 2(b), the D line of

$A(D,C)_2$ splits into two lines of approximately equal intensity. Under [110] stress [Fig. 2(c)], the D line of $A(D,C)_2$ evolves into four lines of approximately equal intensity.

The stress-induced shifts of the $A(D,C)_2$ D transitions are shown in Fig. 3. For [111] stress, under which final-state splitting is negligible, $D_1$ and $D_2$ arise from (1s)-like levels which shift differently. The linear shifts of the respective levels are indicated, and form approximately a 1:3 ratio (see Table II). Under [100] stress, where splitting of the final-state level gives rise to the observed separation $D_2 - D_1$, the level $A(D,C)_2$ remains unaffected, as illustrated in Fig. 3 by the linear shift of nearly zero (see Table II). For [110] stress, under which splitting of the final-state level causes the observed separations $D_4 - D_3 = D_2 - D_1$, the level $A(D,C)_2$ evolves into two levels. Their linear shifts, as indicated in Fig. 3, are approxiately equal and opposite, and have magnitude close to half that of the line $D_2$ which evolves under [111] stress (see Table II). All of the stress-induced shifts of $A(D,C)_2$ are quantitatively consistent with different orientations of trigonal centers[31] in which the hydrostatic shift of (1s)-like levels approximately equals that of p-like levels [a condition which is fulfilled as well by the complexes A(H,Si), A(Be,H) and A(Zn,H)].

The PTI spectra of the D transitions of $A(H,Si)_1$ and $A(H,Si)_2$, as well as aluminum, are shown in Fig. 4. These spectra are slightly alloy-broadened, because the sample was intentionally doped with silicon.[32] In a manner very similar to $A(D,C)_2$, the D line of $A(H,Si)_2$ evolves into two peaks, $D_1[2]$ and $D_2[2]$, whose relative intensities form approxiately a 3:1 ratio. In addition, the D line of $A(H,Si)_1$ splits into two lines, $D_1[1]$ and $D_2[1]$, with shifts and relative intensities that are respectively the approximate "mirror images" of

$D_2[2]$ and $D_1[2]$. The intensity ratio $D_1[1]:D_2[1]$ is expected to be somewhat smaller than $D_2[2]:D_1[2]$ because of stress-induced changes in thermal population (see Section IV.B).

The energies of the A(H,Si) D lines under [111] compression are shown in Fig. 5. Linear least-squares fits to the observed peak positions yield directly the energy shifts of the (1s)-like levels, as indicated there. The lines $D_2[1]$ and $D_1[2]$ are expected on theoretical grounds to exhibit shifts which are nonlinear in stress (see Section IV.B.1 below), but the present data are insufficient to make possible a meaningful nonlinear fit. It is clear from Fig. 5 that the observed linear shifts of $D_2[1]$ and $D_1[2]$ are opposite in sign and of nearly equal magnitude; the same is true of $D_1[1]$ relative to $D_2[2]$ (see Table II). These energy shifts, together with the relative intensities shown in Fig. 4, indicate that the A(H,Si) complex has trigonal symmetry.[31]

### C. Piezospectroscopic studies of A(Be,H) and A(Zn,H)

Figure 6 shows the D transitions of $A(Be,H)_1$ and $A(Be,H)_2$, as well as boron and aluminum, under [111] compression. The D line of the ground-state level $A(Be,H)_1$ splits into two peaks $D_1[1]$ and $D_2[1]$, whose relative intensities form approximately a 1:3 ratio, and whose shifts form approximately a 3:1 ratio. The D line of $A(Be,H)_2$ also splits into two peaks $D_1[2]$ and $D_2[2]$, whose relative intensities and shifts appear to be approximate "mirror images" of $D_2[1]$ and $D_1[1]$, respectively (interference from $D_2[B]$ makes difficult the measurement of the shifts and intensities of $D_2[2]$). The shifts of the four D lines directly reflect shifts of the (1s)-like levels which evolve from $A(Be,H)_1$ and $A(Be,H)_2$. The results of linear least-squares fits are given in Table II, and are consistent with differently oriented trigonal centers.[31] Although theory predicts

that the lines $D_2$[1] and $D_1$[2] should shift in a nonlinear fashion (see Section IV.B.1 below), the existing data are not sufficient for a nonlinear fit. Comparison of Figs. 2, 4 and 6 shows that under [111] stress, the shifts of the (1s)-like levels of A(Be,H) are opposite in sign to those of the corresponding levels of A(D,C) and A(H,Si).

PTI spectra of A(Zn,H) under stress have already been published,[3] and show that the ground-state (1s)-like level evolves into two levels with shifts (see Table II) and relative intensities which are consistent with different orientations of trigonal centers.[31] We note that the shifts of A(Zn,H) are of the same sign as those of the ground-state level $A(Be,H)_1$, and of sign opposite to those of the ground-state levels of A(D,C) and A(H,Si). It has already been mentioned that the second (1s)-like level of the zinc-hydrogen complex cannot be thermally populated at a temperature below which that acceptor becomes significantly ionized.

## IV. THEORY OF THE PIEZOSPECTROSCOPY OF SHALLOW ACCEPTORS

### A. Tetrahedral centers

The trigonal, hydrogen-related acceptor complexes will be shown to be weakly perturbed tetrahedral acceptors. Therefore we begin with a discussion of the piezospectroscopic behavior of tetrahedral centers.[33-36] A uniform uniaxial stress T (defined to be negative for compression) results in a strain, described by a symmetric, second-rank tensor $\epsilon_{ij}$. For cubic systems, $\epsilon_{ij}$ is given by:

$$\varepsilon_{xx} = T[s_{11}n_x^2 + s_{12}(n_y^2 + n_z^2)]$$

$$\varepsilon_{yy} = T[s_{11}n_y^2 + s_{12}(n_x^2 + n_z^2)] \qquad (3)$$

$$\varepsilon_{zz} = T[s_{11}n_z^2 + s_{12}(n_x^2 + n_y^2)]$$

$$\varepsilon_{ij} = \frac{1}{2}Ts_{44}n_i n_j \ , \quad i = j \ .$$

Here, the $s_{ij}$ are the elastic compliance coefficients of the crystal. The force which generates the stress is oriented with direction cosines $(n_x, n_y, n_z)$ relative to the crystal cubic axes.

In germanium, the valence-band maximum (of angular momentum J = 3/2) is fourfold degenerate, and the four basis states[37] generate the representation $\Gamma_8^+(O_h)$. [We neglect here the split-off band (J = 1/2), separated by a spin-orbit splitting much larger than the scale of any effects considered here.] Uniform strain induces a perturbation of the valence-band maximum described by the Hamiltonian:

$$H(\varepsilon) = -a\varepsilon I - b \ (\varepsilon_{xx}J_x^2 + \varepsilon_{yy}J_y^2 + \varepsilon_{zz}J_z^2 - \frac{5}{4}\varepsilon I) - \frac{2d}{\sqrt{3}} \left\{ \varepsilon_{xy}[J_xJ_y] + \varepsilon_{xz}[J_xJ_z] + \varepsilon_{yz}[J_yJ_z] \right\} . \qquad (4)$$

Here, $\varepsilon = \varepsilon_{xx} + \varepsilon_{yy} + \varepsilon_{zz}$, the $J_i$ are the angular momentum matrices for J = 3/2, I is a 4 x 4 unit matrix, and $[A_iB_j] = (1/2)(A_iB_j + A_jB_i)$. The constants a, b and d are the deformation potentials, representing changes in energy per unit strain. [We find it convenient here to use electron energy, equal to hole binding energy, rather than the hole energy used by some authors.[33-35] As a result, some of our equations have different algebraic signs, but all parameters (e.g., a, b, d, T) are taken to have the same signs

as used by those authors.] Diagonalization of (4) yields the energies:

$$E(\varepsilon) = -a\varepsilon \pm \left\{ \frac{1}{2} b^2 \left[(\varepsilon_{xx} - \varepsilon_{yy})^2 + (\varepsilon_{xx} - \varepsilon_{zz})^2 + (\varepsilon_{yy} - \varepsilon_{zz})^2\right] + d^2 \left(\varepsilon_{xy}{}^2 + \varepsilon_{xz}{}^2 + \varepsilon_{yz}{}^2\right) \right\}^{\frac{1}{2}} . \tag{5}$$

The uniaxial stress creates a hydrostatic shift $-a\varepsilon$, as well as a splitting, discussed in detail below.

For a shallow impurity level of $\Gamma_8(\overline{T}_d)$ symmetry, the linear behavior under stress is described by (4) and (5), with the substitutions $a \rightarrow a'$, $b \rightarrow b'$ and $d \rightarrow d'$. Within the effective-mass theory, $a = a'$ for all s- and p-like acceptor levels. Accordingly, we observe no linear shift of the center of gravity of transitions from strain-split $\Gamma_8(\overline{T}_d)$ acceptor levels; we set to zero the hydrostatic shift in all that follows. In principle, the effective-mass theory allows one to calculate[26,36] b' and d' in terms of b and d for free holes. The envelope function of a given p-like acceptor state is virtually unchanged from one shallow acceptor species to another; we expect the same b' and d' to describe its behavior, independent of the identity of the acceptor. In contrast, the envelope functions of s-like states vary from one species to another, so that in principle, b' and d' will differ for the ground state of each different acceptor. In general equations below, we use the symbols b and d, with the understanding that in numerical calculations, appropriate values of b' and d' are employed.

The linear shifts of the sublevels which evolve under stress from a $\Gamma_8(\overline{T}_d)$ level can be calculated from (3) and (5), and are given in Table III for stresses along the three major crystallographic directions. That table

also indicates how the $\Gamma_8(\overline{T}_d)$ level decomposes into the irreducible representations of the reduced-symmetry point groups. In the experimental stress calibrations described in (1) and (2), $\Delta_1^{Ga}$ was obtained for a given stress direction using the difference of the two shifts, substituting in the expressions of Table III the values[26] $b'_{Ga} = -1.33 \pm 0.03$ eV, $d'_{Ga} = -2.91 \pm 0.06$ eV. Similarly, $\Delta_1^D$ was obtained by making use of $b'_D = 0.60 \pm 0.10$ eV, $d'_D = 0.00 \pm 0.06$ eV. We employed the values[27] $s_{11} = 9.585 \times 10^{-4}$ kbar$^{-1}$, $s_{12} = -2.609 \times 10^{-4}$ kbar$^{-1}$ and $s_{44} = 14.542 \times 10^{-4}$ kbar$^{-1}$.

## B. Reduced-symmetry centers

It is generally difficult to perform a first-principles calculation of the electronic structure of a reduced-symmetry defect complex with sufficient accuracy for detailed comparison with spectroscopic data. As we show here, there exist cases in which a shallow acceptor of reduced symmetry can be represented reasonably by a tetrahedral center, plus a small perturbation localized in the central cell region. That perturbation splits the fourfold-degenerate (1s)-like ground-state level into two Kramers doublet levels, and leaves the p-like levels essentially unchanged.[38]

In order to describe the piezospectroscopic behavior of the (1s)-like levels of a reduced-symmetry shallow acceptor, we begin with a hypothetical tetrahedral acceptor which models as closely as possible the reduced-symmetry center.[39] In the fourfold basis for the $\Gamma_8(\overline{T}_d)$ acceptor level,[37] we describe the reduction of symmetry by a Hamiltonian $H^k_{red}$, where the superscript k ranges over the N different orientations of centers in the lattice. Diagonalization of $H^k_{red}$ alone would yield the zero-stress splitting between the two (1s)-like levels, the same for all N orientations. Returning to the hypothetical tetrahedral acceptor, we assume its linear behavior under stress is described by (4), with known values of b' and d'. Then the piezospectroscopic behavior

of the reduced-symmetry center is obtained by diagonalization of the total Hamiltonian:

$$H^k_{tot} = H^k_{red} + H(\varepsilon) \ . \tag{6}$$

The eigenvalues of $H^k_{tot}$ will in general be different for the various orientations k, corresponding to[31] the "lifting of orientational degeneracy".

We choose a hypothetical tetrahedral acceptor whose (1s)-like level lies midway between the zero-stress positions of the two (1s)-like levels of the reduced-symmetry acceptor, so that $H^k_{red}$ has zero trace. Then the elements of $H^k_{red}$ depend on only one (trigonal and tetragonal centers) or two (rhombic I centers) parameter(s), and are related to one another in a well defined way by symmetry considerations (and for rhombic I centers by the defect's degree of tetragonal character; see Section IV.B.2). We model the symmetry reduction represented by $H^k_{red}$ using one (or two) uniaxial stress(es), uniform in magnitude throughout the entire crystal, which result in equivalent symmetry reduction and splitting between the two (1s)-like levels. In the case of a trigonal center, for example, we employ a stress oriented along the $C_3$ axis of the complex. We do not imply that the actual trigonal distortion takes the form of a uniform stress or even necessarily a local stress; the equivalent "internal stress" is merely a computational device to obtain the matrix elements of $H^k_{red}$ and to simplify subsequent diagonalization of $H^k_{tot}$.

From the equivalent "internal stress", we obtain the corresponding "internal strain" tensor $\varepsilon^k_{int}$ using (3). Then (4) allows us to derive the internal strain perturbation $H(\varepsilon^k_{int})$, equivalent[40] to $H^k_{red}$. The strain produced by externally applied stress is now denoted by $\varepsilon_{ext}$; under such stress, the total Hamiltonian becomes:

$$H^k_{tot} = H(\varepsilon^k_{int}) + H(\varepsilon_{ext}) \ . \tag{7}$$

Since (4) is linear in strain, we can write:

$$H^k_{tot} = H(\varepsilon^k_{tot}) \ , \tag{8}$$

with

$$\varepsilon^k_{tot} = \varepsilon^k_{int} + \varepsilon_{ext} \ , \tag{9}$$

and obtain the eigenvalues of (8) by substitution into (5).

The observed intensities of optical transitions at reduced-symmetry centers under stress are dependent upon several factors. The intensities of transitions from a given initial-state energy depends upon the number of defect orientations which have a (1s)-like level at that energy, i.e., the degree of "orientational degeneracy" remaining under stress. The relative intensities of the transitions from the two (1s)-like levels of a given orientation are modified as the occupation of the two levels changes under stress; the relevant Boltzmann factor is altered according to the stress-dependent energy separation of the two levels. We do not derive here the polarization dependence of the intensities of optical transitions. We note that according to symmetry-derived electric-dipole selection rules, unpolarized radiation permits observation of transitions from both (1s)-like levels, to both of the sublevels which evolve under stress from a $\Gamma_8(\overline{T}_d)$ p-like level, for all orientations of all classes of reduced symmetry considered here.

We remark that at high stresses, the present theory must be modified to include a quadratic shift of the (1s) multiplet.[36] In addition, it must

include interaction between (1s)-like levels and nearby p-like levels. The latter effect does not occur appreciably below 3 kbar in tetrahedral shallow acceptors,[36] but could occur at applied stresses of lower magnitude when $H^k_{red}$ pushes the zero-stress position of the excited (1s)-like level closer to the p-like levels. The present theory assumes that the externally applied stress does not alter $H^k_{red}$, such as by causing reorientation of the complexes.

### 1. Trigonal centers

We label the four orientations of trigonal ($\overline{C}_{3v}$) acceptor complexes according to the direction of the $C_3$ axis (see Table IV), and model the corresponding trigonal distortion by an equivalent "internal stress" S directed along that axis. The magnitude of S is chosen to reproduce the observed zero-stress separation between the two (1s)-like levels; factors which govern the choice of the sign of S will become apparent. We now present the (1s)-like energy levels of the four different orientations of trigonal acceptor complexes. (Recall that T denotes the magnitude of the externally applied stress.)

<u>No externally applied stress</u>:

I, II, III, IV: $$E = \pm \frac{\sqrt{3}}{6} ds_{44} S \tag{10}$$

<u>Stress applied along [111]:</u>

I: $$E = \pm \frac{\sqrt{3}}{6} ds_{44}(S + T) \tag{11}$$

II, III, IV: $$E = \pm \frac{\sqrt{3}}{6} ds_{44}(S^2 - \tfrac{2}{3}ST + T^2)^{\frac{1}{2}} \tag{12}$$

Stress applied along [100]:

$$\text{I, II, III, IV:} \quad E = \pm \left[\frac{1}{12}(ds_{44})^2 S^2 + b^2(s_{11} - s_{12})^2 T^2\right]^{\frac{1}{2}} \tag{13}$$

Stress applied along [110]:

$$\text{I, IV:} \quad E = \pm\left[\frac{1}{12}(ds_{44})^2 S^2 + \frac{1}{12}(ds_{44})^2 ST + \frac{1}{4}b^2(s_{11} - s_{12})^2 T^2 + \frac{1}{16}(ds_{44})^2 T^2\right]^{\frac{1}{2}} \tag{14}$$

$$\text{II, III:} \quad E = \pm \left[\frac{1}{12}(ds_{44})^2 S^2 - \frac{1}{12}(ds_{44})^2 ST + \frac{1}{4}b^2(s_{11} - s_{12})^2 T^2 + \frac{1}{16}(ds_{44})^2 T^2\right]^{\frac{1}{2}} \tag{15}$$

The general features of these equations are illustrated in Fig. 7. Those curves have been calculated using[26] $b = b'_{Ga}$ and $d = d'_{Ga}$ (see Section IV.A), and $T < 0$ corresponding to externally applied uniaxial compression. [The values of S, +0.205 kbar and -0.810 kbar, have been chosen to fit the properties of A(Be,H) and A(D,C) respectively (see Section IV.C).] To the left of each graph, we indicate the representations of $\overline{C}_{3v}$ according to which the acceptor levels transform in the absence of externally applied stress, obtained by comparison of (10) with Table III. Comparing Figs. 7(a) and 7(b), we note that changing the sign of S reverses the ordering of the $\Lambda_4$ and $\Lambda_{5,6}$ levels. As a result, the two levels of orientation I move toward each other under [111] compression in Fig. 7(a), and away from each other in Fig. 7(b); the response to small [111] stress of the levels of orientations II-IV is similarly reversed. For orientation I under [111] stress, the point group remains $\overline{C}_{3v}$ and the two levels, of different symmetries, do not interact. In all other cases, stress reduces the point groups to $\overline{C}_{1h}$; because that group

has only two singlet complex representations which are degenerate by time reversal symmetry the two levels do not cross, and exhibit nonlinear shifts.

If we expand (11)-(15) and keep terms only to linear order in T/S, we can show that these small-stress linear shifts depend only on the deformation potential parameter d, and are independent of the magnitude of S. Under [111] stress, the shifts of orientation I are $\pm(\sqrt{3}/6)ds_{44}T$, identical in magnitude to the shifts of the sublevels which evolve under [111] stress from a $\Gamma_8(\overline{T}_d)$ level (see Table III); for a given (1s)-like level, the shifts of orientations II-IV are $(-1/3)[\pm(\sqrt{3}/6)ds_{44}T]$. Under [100] stress, the small-stress linear shifts of all orientations are zero. Finally, under [110] stress, the small-stress linear shifts of orientations I and IV are $(1/2)[\pm(\sqrt{3}/6)ds_{44}T]$, while those of orientations II and III are $(-1/2)[\pm(\sqrt{3}/6)ds_{44}T]$. All of these shifts are consistent with the generally permissible small-stress linear behavior of trigonal centers in which there is no hydrostatic shift of transition energies.[31]

Comparison of (11)-(15) with Table III shows that all of the high-stress shifts have slopes equal to those of the sublevels which evolve from a $\Gamma_8(\overline{T}_d)$ level under stresses along the respective directions. If we reverse the labeling of the two zero-stress sublevels and rescale the stress and energy axes, then Figure 7(a) indicates the behavior under uniaxial tension of the acceptor described in Fig. 7(b) (and vice-versa).

## 2. Tetragonal and rhombic I centers

In this section, we extend the theory to predict the piezospectroscopic behavior of tetragonal and rhombic I shallow acceptor complexes in germanium,

in case such complexes should be observed in the future. A tetragonal ($\overline{D}_{2d}$) complex has an $S_4$ axis directed along a <100> direction, so that such complexes have three possible orientations in the lattice. The reduction from tetrahedral to tetragonal symmetry may be represented by an equivalent "internal stress" P, directed along the $S_4$ <100> axis. It is possible to transform a tetragonal center to a rhombic I ($\overline{C}_{2v}$) center by transforming the $S_4$ axis into a $C_2$ axis; we do that here by application of an "internal stress" Q along a <110> direction perpendicular to the <100> $S_4$ axis. We label the six possible orientations of rhombic I complexes as indicated in Table V. In the tetragonal limit (Q = 0), orientations I, II, III are equivalent to IV, V, VI, respectively.

In order to calculate the piezospectroscopic behavior of a given orientation, we use (3) to obtain the "internal strain" tensor $\varepsilon^k_{int}$ which results from a superposition of the stresses P and Q. We combine the resulting $\varepsilon^k_{int}$ with $\varepsilon_{ext}$, the strain tensor corresponding to externally applied stress, to obtain $\varepsilon^k_{tot}$, and obtain the energy levels by substitution of $\varepsilon^k_{tot}$ into (5). Tetragonal centers can be obtained as a special case of our results. In presenting the energy levels, we define the following energy parameter:

$$\Delta = [b^2(s_{11} - s_{12})^2(P - \tfrac{1}{2}Q)^2 + \tfrac{1}{16}(ds_{44})^2Q^2]^{\frac{1}{2}} \tag{16}$$

<u>No externally applied stress:</u>

I, II, III, IV, V, VI: $$E = \pm\Delta \tag{17}$$

<u>Stress applied along [111]:</u>

I, II, III: $$E = \pm[\Delta^2 + \tfrac{1}{12}(ds_{44})^2(QT + T^2)]^{\frac{1}{2}} \tag{18}$$

IV, V, VI: $$E = \pm[\Delta^2 + \frac{1}{12}(ds_{44})^2(-QT + T^2)]^{\frac{1}{2}} \tag{19}$$

<u>Stress applied along [100]:</u>

I, IV: $$E = \pm [\Delta^2 + b^2(s_{11} - s_{12})^2(2PT - QT + T^2)]^{\frac{1}{2}} \tag{20}$$

II, III, V, VI: $$E = \pm [\Delta^2 + b^2(s_{11} - s_{12})^2(-PT + \frac{1}{2}QT + T^2)]^{\frac{1}{2}} \tag{21}$$

<u>Stress applied along [110]:</u>

I, II, IV, V: $$E = \pm [\Delta^2 + b^2(s_{11} - s_{12})^2(\frac{1}{2}PT - \frac{1}{4}QT + \frac{1}{4}T^2) + \frac{1}{16}(ds_{44})^2T^2]^{\frac{1}{2}} \tag{22}$$

III: $$E = \pm [\Delta^2 + b^2(s_{11} - s_{12})^2(-PT + \frac{1}{2}QT + \frac{1}{4}T^2) + \frac{1}{16}(ds_{44})^2(2QT + T^2)]^{\frac{1}{2}} \tag{23}$$

VI: $$E = \pm [\Delta^2 + b^2(s_{11} - s_{12})^2(-PT + \frac{1}{2}QT + \frac{1}{4}T^2) + \frac{1}{16}(ds_{44})^2(-2QT + T^2)]^{\frac{1}{2}} \tag{24}$$

We discuss first the tetragonal ($Q = 0$) limit. In that case, the two levels have $X_6$ and $X_7(\overline{D}_{2d})$ symmetry, and changing the sign of P reverses their ordering. The small-stress linear shifts (those to linear order in T/P) depend

only on the deformation potential b, and are independent of the magnitude of P. Under [111] stress, the shifts are zero for all orientations. Under [100] stress, orientation I has a shift of $\pm b(s_{11} - s_{12})T$, equal in magnitude to the shift of the sublevels which evolve from a $\Gamma_8(\overline{T}_d)$ under [100] stress (see Table III); orientations II and III have shifts of $(-1/2)[\pm b(s_{11} - s_{12})T]$. Under [110] stress, orientations I and II have shifts of $(1/4)[\pm b(s_{11} - s_{12})T]$, while orientation III has a shift of $(-1/2)[\pm b(s_{11} - s_{12})T]$. All of these small-stress linear shifts are consistent with the generally allowed behavior of tetragonal centers which do not exhibit a hydrostatic shift of transition energies.[31]

The response of rhombic I shallow acceptor complexes to uniaxial compression is illustrated in Fig. 8. Those curves have been calculated using[26] $b = b'_{Ga}$ and $d = d'_{Ga}$ (see Section IV.A). The values of P and Q have been chosen so that $P = 4Q$, representing nearly tetragonal centers; P and Q are positive in Fig. 8(a) and negative in Fig. 8(b). In the absence of externally applied stress, the two levels have $\Delta_5(\overline{C}_{2v})$ symmetry. We note that in Fig. 8(a), an avoided crossing is predicted under [100] stress. In the tetragonal limit, orientation I (equivalent to orientation IV) would retain $\overline{D}_{2d}$ symmetry under [100] stress and the two levels, of different symmetries, would cross. But with the rhombic distortion, both levels have $\Delta_5(\overline{C}_{2v})$ symmetry under [100] stress, and are forbidden to cross.

It can easily be shown that in the general rhombic I case, this theory predicts shifts to linear order in T/P and T/Q which do depend on the magnitudes of P and Q, and which are consistent with the generally permissible behavior of rhombic I centers which have no hydrostatic shift of transition energies.[31] For both tetragonal and rhombic I centers, the slopes of the high-

stress shifts are equal to those of the levels which evolve from a $\Gamma_8(\overline{T}_d)$ level under stresses along the respective directions. We note that with reversed labeling of the $X_6$ and $X_7$ levels, Fig. 8(a) describes the behavior under tension of the acceptor whose behavior under compression is described by Fig. 8(b) (and vice-versa).

### C. Application to hydrogen-related trigonal centers

We apply here the theory developed in Section IV.B.1 to the experimental data presented in Sections III.B and III.C. Examination of Table I shows that for A(D,C), A(H,Si) and A(Be,H), the average binding energy of the two (1s)-like levels lies fairly close to 11.32 meV, the value for gallium.[18,25] The average energy of the two (1s)-like levels of A(Zn,H) is not known. We attempt to describe all four trigonal, hydrogen-related centers using the values[26] $b = b'_{Ga}$ and $d = d'_{Ga}$ (see Section IV.A) in evaluation of the expressions (10)-(15).

Comparison of the theory to the experimentally observed [111] stress shifts indicates that we have to choose a negative value of S to describe A(D,C) and A(H,Si), and a posivive value of S for A(Be,H) and A(Zn,H). For the first three of these complexes, we choose the magnitude of S to reproduce the zero-stress spacing of the two (1s)-like levels (see Table I). In the case of A(Zn,H), choice of an arbitrary positive S results in unambiguous prediction of the small-stress linear shifts. The large zero-stress separation between the two (1s)-like levels implies a large value of S; we therefore expect the stress-induced shifts to be essentially linear over the range of stress values that have been employed in experimental study of A(Zn,H) (up to 0.11 kbar). Complete predictions of the piezospectroscopic behavior of A(Be,H) and A(D,C) are illustrated in Figs. 7(a) and 7(b), respectively; the qualitative features have already been discussed in Section IV.B.1.

In Table VI, we present a summary of the values of S employed to describe the trigonal, hydrogen-related complexes, and give the representations of $\overline{C}_{3v}$ according to which the acceptor levels transform in the absence of applied stress. In all cases where experimental data is available for comparison, we present the theoretical small-stress linear shifts of the acceptor levels, obtained by evaluation of (11)-(15) to linear order in T/S. We also list the deviations of experimental data from the theory. For A(H,Si) and A(Be,H), the zero-stress separation of the two (1s)-like levels is small enough that at the stresses used in our experiments, we expect the levels of orientations II-IV to exhibit shifts which are nonlinear in stress. We have evaluated the nonlinear theoretical expression (12) at the stress values used to record spectra under [111] stress, and have performed a linear least-squares fit to the energies thus calculated. The resulting shifts have been included in Table VI in parentheses; they are generally in better agreement with experiment than direct evaluation of a linearized form of (12).

## V. DISCUSSION

For a static impurity complex in the diamond lattice which has two constituents, one of which is substitutional and the other of which is interstitial, the highest symmetry possible is trigonal. Our piezospectroscopic studies of the four hydrogen-related acceptor complexes reveal energy shifts and relative intensities which are the clear signatures of trigonal structures. It can be seen in Table VI that the theory developed in Section IV.B.1 is generally in good quantitative agreement with the experimentally determined shifts of (1s)-like levels. The experimental uncertainties discussed in Section II, including errors in sample alignment and calibration of stress values, could easily be large enough to explain most of the discrepancies evident in Table VI. An

additional possible source of disagreement lies in our use of $b'_{Ga}$ and $d'_{Ga}$ to describe the piezospectroscopic behavior of all four complexes. We feel that this choice is more appealing than the introduction of additional adjustable parameters. The poorest agreement between experiment and theory exists for orientations II-IV of A(Zn,H) under [111] stress. Since that center has the largest zero-stress separation between (1s)-like levels, it is the most strongly perturbed from tetrahedral symmetry. Our treatment might be least valid in this case.

The present theory makes definite predictions of the nonlinear stress-dependent shifts of trigonal centers. Those predictions have been tested only partially here, in that they provide an improved explanation of the apparently linear shifts for A(H,Si) and A(Be,H). Because it has a small zero-stress separation of (1s)-like levels, the acceptor A(Be,H) might allow study of nonlinear behavior at stresses below which the (1s)-like levels interact strongly with p-like levels. An accurate theoretical description of these four trigonal complexes at stresses above approximately 2 kbar might be achieved by extension of the recent work of Broeckx and Vennik[36] to include a zero-stress trigonal perturbation for (1s)-like states.

Besides the four trigonal, hydrogen-related complexes, at least two other shallow acceptor species in germanium are known to possess two (1s)-like levels (see Table I). The present work suggests that each of these centers probably has a class of symmetry lower than tetrahedral. It might be interesting to see if either acceptor center has tetragonal or rhombic I symmetry, and can thus serve to test the theory presented in Section IV.B.2.

In terms of its overall effect on the electrical activity of impurity complexes in which it is included, hydrogen can have one of two qualitatively

opposite effects. First, a (H,X) complex may have electrical behavior equivalent to a substitutional atom which lies in the periodic table one column to the left of the atom X. Examples of this case are A(H,C) and A(H,Si) in germanium,[1] D(H,O) in germanium,[15], D(H,S) in silicon,[41] and electrically inactive (H,P) complexes in silicon.[9] In terms of the extreme ionic limit, we might say that "H behaves as $H^-$", accepting a second electron into its (1s) orbital. The resulting Coulomb repulsion would be energetically unfavorable,[42] providing a qualitative explanation for the generally low thermal stability of this class of complexes.

In the second case, a (X,H) complex may behave electrically like a substitutional atom which lies in the periodic table one column to the right of the atom X. Ionically speaking, we might say that "H behaves as H+", donating an electron to the deficient bonding environment of the atom X. The resulting proton would be Coulombically attracted to the negatively charged $X^-$ ion, explaining qualitatively the generally greater stability of these complexes. Examples include A(Be,H) and A(Zn,H) in germanium,[3] A(Be,H) and A(Be,D) in silicon,[20] A(Cu,Y,Z) in germanium,[21] with Y,Z = H,D,T, and passivated (B,H) complexes in silicon.[6-8]

In fitting the observed piezospectroscopic behavior of the four trigonal, hydrogen-related acceptor complexes in germanium (see Section IV.C), it was necessary to use a negative value of S for A(D,C) and A(H,Si), and a positive value of S for A(Be,H) and A(Zn,H). It is likely that this reversal of the trigonal distortion is related to the different role which hydrogen plays in determining the electrical activity of the first two centers, as compared to the second two. The acceptors A(D,C) and A(H,Si) might thereby be equivalent to tetrahedral acceptors perturbed by electric dipoles pointing along antibonding directions, while A(Be,H) and A(Zn,H) would be perturbed by dipoles pointing along bonding directions.

The isotope shift of transition energies[14] which has been observed upon deuteration of A(H,Si) was previously explained in terms of the tunneling of the light nuclei.[1] In view of the evidence presented here, the isotope shift must instead be interpreted in terms of a vibrational mode of those nuclei, coupled to the bound hole. A theory along such lines has already been proposed,[43] and yields an isotope shift of the correct order of magnitude.

We should contrast the four trigonal, hydrogen-related acceptor complexes in germanium with A(Be,H) and A(Be,D) in silicon,[20] which have been explained in terms of the rapid tunneling of the light nuclei[1] with millielectronvolt energies. We recall that the tunneling rate t essentially scales as[44]:

$$t \sim \exp(-\alpha m^{\frac{1}{2}}) \ , \tag{25}$$

where m is the mass of the tunneling particle and $\alpha$ depends on its kinetic energy and on the potential in which it moves. The tunneling rate can be drastically affected by the changes in $\alpha$ which accompany the change from one host crystal to another. It has been demonstrated that the dynamic properties of semiconductor defects can also be altered dramatically by small changes in hydrogen isotopic mass.[21] It seems unlikely that current theoretical techniques have sufficient accuracy to calculate tunneling rates from first principles.

## ACKNOWLEDGEMENTS

We are grateful to D. D. Nolte and W. Walukiewicz for informative discussions. This work was supported by National Science Foundation Grant No. DMR-85-02502 and, at the Lawrence Berkeley Laboratory, by the Director's Office of Energy Research, U.S. Department of Energy under Contract No. DE-AC03-76SF00098.

*Present address: AT&T Bell Laboratories, Crawford Hill Laboratory, Holmdel, New Jersey 07733.

[1]E. E. Haller, B. Joós, and L. M. Falicov, Phys. Rev. B21, 4729 (1980).

[2]Sh. M. Kogan and T. M. Lifshits, Phys. Stat. Sol. (a) 39, 11 (1977).

[3]R. E. McMurray, Jr., N. M. Haegel, J. M. Kahn, and E. E. Haller, Solid State Commun. 61, 27 (1987).

[4]S. J. Pearton and A. J. Tavendale, Phys. Rev. B26, 7105 (1982).

[5]S. J. Pearton, J. M. Kahn, W. L. Hansen, and E. E. Haller, J. Appl. Phys. 55, 1464 (1984).

[6]J. I. Pankove, D. E. Carlson, J. E. Berkeyheiser, and R. O. Wance, Phys. Rev. Lett. 51, 2224 (1983). See also: J. I Pankove, R. O. Wance, and J. E. Berkeyheiser, Appl. Phys. Lett. 45, 1100 (1984); and J. I. Pankove, P. J. Zanzucchi, C. W. Magee, and G. Lucovsky, Appl. Phys. Lett. 46, 421 (1985).

[7]G. G. DeLeo and W. B. Fowler, Phys. Rev. B31, 6861 (1985).

[8]L. V. C. Assali and J. R. Leite, Phys. Rev. Lett. 55, 980 (1985). See also: G. G. DeLeo and W. B. Fowler, Phys. Rev. Lett. 56, 402 (1986); and L. V. C. Assali and J. R. Leite, Phys. Rev. Lett. 56, 403 (1986).

[9]N. M. Johnson, C. Herring, and D. J. Chadi, Phys. Rev. Lett. 56, 769 (1986).

[10]E. E. Haller, W. L. Hansen, and F. S. Goulding, Adv. Phys. 30, 93 (1981).

[11]E. E. Haller, "Semiconductor Physics in Ultra-Pure Germanium", in: Festkörperprobleme 26, 203, P. Grosse, ed. (Vieweg, Braunschweig, 1986).

[12]W. L. Hansen, E. E. Haller, and P. N. Luke, IEEE Trans. Nucl. Sci. NS-29, 738 (1982).

[13]R. N. Hall, IEEE Trans. Nucl. Sci. NS-21, 260 (1974).

[14]E. E. Haller, Phys. Rev. Lett. 40, 584 (1978).

[15]B. Joós, E. E. Haller, and L. M. Falicov, Phys. Rev. B22, 832 (1980).

[16]E. E. Haller and R. E. McMurray, Jr., Physica 116 B+C, 349 (1983).

[17]L. S. Darken, J. Appl. Phys. 53, 3754 (1982).

[18]A. Baldereschi and N. O. Lipari, Physics of Semiconductors, F. G. Fumi, ed. (Proc. of the 13th Intl. Conf., Marves, Rome, 1976), p. 595.

[19]We label the irreducible representations according to the notation of: G. F. Koster, "Space Groups and Their Representations", in: Solid State Physics, vol. 5., F. Seitz and D. Turnbull, eds. (Academic, New York, 1957), p. 173.

[20]K. Muro and A. J. Sievers, Phys. Rev. Lett. 57, 897 (1986).

[21]J. M. Kahn, L. M. Falicov, and E. E. Haller, Phys. Rev. Lett. 57, 2077 (1986).

[22]Y. Yamada, A. Mitsuishi, and H. Yoshinaga, J. Opt. Soc. Amer. 52, 17 (1962).

[23]J. M. Kahn, "Hydrogen-Related Acceptor Complexes in Germanium", PhD Thesis, Department of Physics, University of California, Berkeley, November, 1987 (unpublished), Lawrence Berkeley Laboratory Report Number 22652.

[24]A. G. Kazanskii, P. L. Richards, and E. E. Haller, Solid State Commun. 24, 603 (1977).

[25]E. E. Haller and W. L. Hansen, Solid State Commun. 15, 687 (1974).

[26]A. D. Martin, P. Fisher, C. A. Freeth, E. H. Salib, and P. E. Simmonds Phys. Lett 99A, 391 (1983).

[27]M. E. Fine, J. Appl. Phys. 26, 862 (1955).

[28]R. L. Jones and P. Fisher, Phys. Rev. B2, 2016 (1970).

[29]The spectra shown in Fig. 2 were recorded during studies of the piezo-spectroscopy of the acceptors $A(Cu,D_2)$ (see Refs. 21 and 23) near ($E_v$ + 18 meV). The samples used had a net excess of shallow donors over shallow

acceptors and became p-type after addition of $A(Cu,D_2)$, so that in equilibrium, all shallower acceptors were ionized by compensation. Free holes photogenerated from $A(Cu,D_2)$ neutralized some shallower acceptors, allowing their observation. However, all shallower acceptors thermally ionized at a temperature sufficient to allow observable population of $A(D,C)_1$, explaining our inability to monitor that level in these spectra.

[30] P. Fisher (private communication).

[31] A. A. Kaplyanskii, Opt. Spectrosc. (USSR), 16, 329 (1964).

[32] To insure survival of a measurable concentration of A(H,Si) after room-temperature handling, the sample was taken from a crystal doped with $\sim 10^{17}$ $cm^{-3}$ silicon (see Ref. 1), leading to the alloy broadening evident in Fig. 4.

[33] G. E. Pikus and G. L. Bir, Sov. Phys. Solid State. 1, 1502 (1960).

[34] G. L. Bir, E. I. Butikov, and G. E. Pikus, J. Phys. Chem. Solids 24, 1467 (1963).

[35] G. L. Bir and G. E. Pikus, Symmetry and Strain-Induced Effects in Semiconductors (John Wiley and Sons, New York, 1974).

[36] J. Broeckx and J. Vennik, Phys. Rev. B35, 6165 (1987).

[37] J. M. Luttinger and W. Kohn, Phys. Rev. 97, 869 (1955).

[38] We observe here that the trigonal distortion does not measurably split the p-like levels and does not measurably alter $b'_D$ and $d'_D$, the deformation potentials of the $2\Gamma_8^-$ level.

[39] We desire that when the strain Hamiltonian of the hypothetical tetrahedral acceptor is diagonalized simultaneously with the structural reduction of symmetry, we obtain the best possible description of the piezospectroscopic behavior of the reduced-symmetry center.

[40]Our choice of a traceless $H^k_{red}$ dictates that we set to zero the hydrostatic shift induced by $\epsilon^k_{int}$.

[41]S. P. Love, K. Muro, R. E. Peale, and A. J. Sievers, Bull. Am. Phys. Soc. Ser. II 32, 438 (1987).

[42]J. Oliva and L. M. Falicov, Phys. Rev. B28, 7366 (1983).

[43]Sh. M. Kogan, Sov. Phys. Semicond. 13, 1131 (1979).

[44]See, for example: Tunneling Phenomena in Solids, E. Burstein and S. Lundqvist, eds. (Plenum, New York, 1969).

TABLE I. Acceptor complexes in germanium with two (1s)-like levels.[a]

| Acceptor Complex | Acceptor Levels and Binding Energy[b] (meV) | | | | Energy Splitting (meV) | Average Energy (meV) |
|---|---|---|---|---|---|---|
| | (1s)-like Ground State | | (1s)-like Excited State | | | |
| A(H,C)[c] | $A(H,C)_2$ | 12.28 | $A(H,C)_1$ | 10.30 | 1.98 | 11.29 |
| A(H,Si)[c] | $A(H,Si)_2$ | 11.66 | $A(H,Si)_1$ | 10.59 | 1.07 | 11.13 |
| A(Be,H)[d] | $A(Be,H)_1$ | 11.29 | $A(Be,H)_2$ | 10.79 | 0.50 | 11.04 |
| A(Zn,H)[d] | A(Zn,H) | 12.53 | e | e | e | e |
| $(A_3/A_5)$[f] | $A_5$ | 11.32 | $A_3$ | 10.22 | 1.10 | 10.77 |
| $(A_{10}/A_{11})$[g] | $A_{11}$ | 12.03 | $A_{10}$ | 11.45 | 0.58 | 11.74 |

[a]This list includes only acceptors with hole binding energies less than 12.6 meV.

[b]All values are subject to an uncertainty of ±0.01 meV.

[c]Ref. 1.

[d]Ref. 3.

[e]A second (1s)-like level has not been detected, but is expected to exist; see text.

[f]Ref. 16.

[g]Ref. 17.

TABLE II. Experimental stress-induced linear shifts[a] of the (1s)-like levels of trigonal acceptor complexes.

| Acceptor Level | Stress Direction | Energy Shifts (mev/kbar) |
|---|---|---|
| $A(D,C)_2$ | [111] | +1.4 ± 0.1 |
| | | -0.36 ± 0.02 |
| | [100] | +0.002 ± 0.004 |
| | [110] | +0.69 ± 0.02 |
| | | -0.644 ± 0.003 |
| $A(H,Si)_2$ | [111] | +1.31 ± 0.02 |
| | | -0.24 ± 0.03 |
| $A(H,Si)_1$ | [111] | +0.272 ± 0.006 |
| | | -1.26 ± 0.04 |
| $A(Be,H)_1$ | [111] | +0.45 ± 0.06 |
| | | -1.17 ± 0.03 |
| $A(Be,H)_2$ | [111] | b |
| | | -0.52 ± 0.06 |
| A(Zn,H) | [111] | +0.594 ± 0.009 |
| | | -1.35 ± 0.05 |

[a]Values given are the shifts of hole binding energy per unit compressional stress, $-\delta E/T$. Errors quoted reflect the standard deviations of the slopes obtained from least-squares analyses of the observed shifts.

[b]Spectral interference precludes quantification of this shift; see text.

Table III. The linear shifts of the stress-induced sublevels which evolve from a $\Gamma_8(\overline{T}_d)$ level. The shifts are given in terms of hole binding energy.

| Stress Direction | Sublevel | Energy Shift |
|---|---|---|
| [111] | $\Lambda_4(\overline{C}_{3v})$ | $+\frac{\sqrt{3}}{6}ds_{44}T$ |
| | $\Lambda_{5,6}(\overline{C}_{3v})$ | $-\frac{\sqrt{3}}{6}ds_{44}T$ |
| [100] | $X_7(\overline{D}_{2d})$ | $+ b(s_{11} - s_{12})T$ |
| | $X_6(\overline{D}_{2d})$ | $- b(s_{11} - s_{12})T$ |
| [110] | $\Delta_5(\overline{C}_{2v})$ | $+ [\frac{1}{4}b^2(s_{11} - s_{12})^2 + \frac{1}{16}(ds_{44})^2]^{\frac{1}{2}} T$ |
| | $\Delta_5(\overline{C}_{2v})$ | $- [\frac{1}{4}b^2(s_{11} - s_{12})^2 + \frac{1}{16}(ds_{44})^2]^{\frac{1}{2}} T$ |

Table IV. The four orientations of trigonal complexes in the diamond lattice.

| Orientation Label | $C_3$ Axis |
|---|---|
| I | [111] |
| II | $[1\bar{1}\bar{1}]$ |
| III | $[\bar{1}1\bar{1}]$ |
| IV | $[\bar{1}\bar{1}1]$ |

Table V. The six orientations of rhombic I complexes in the diamond lattice.

| Orientation Label | <100> $C_2$ Axis (P) | <110> Axis (Q) Perpendicular to $C_2$ Axis |
|---|---|---|
| I | [100] | [011] |
| II | [010] | [101] |
| III | [001] | [110] |
| IV | [100] | $[01\bar{1}]$ |
| V | [010] | $[10\bar{1}]$ |
| VI | [001] | $[1\bar{1}0]$ |

TABLE VI. The linear shifts[a] of the (1s)-like levels of trigonal acceptor complexes: comparison of theory to experiment.

| Equivalent Stress S (kbar) | Acceptor Level | $(\bar{C}_{3v})$[b] | Stress Direction | Orientation Label(s) | Theoretical Energy Shift (meV/kbar) | Deviation of Experiment from Theory (%)[c] |
|---|---|---|---|---|---|---|
| -0.810 | $A(D,C)_2$ | $\Lambda_4$ | [111] | I | +1.222 | +15 |
| | | | | II-IV | -0.407 | -12 |
| | | | [100] | I-IV | 0 | d |
| | | | [110] | I,IV | +0.611 | +13 |
| | | | | II,III | -0.611 | + 5 |
| | $A(D,C)_1$ | $\Lambda_{5,6}$ | e | e | e | e |
| -0.438 | $A(H,Si)_2$ | $\Lambda_4$ | [111] | I | +1.222 | + 7 |
| | | | | II-IV | -0.407(-0.240[f]) | -41(0[f]) |
| | $A(H,Si)_1$ | $\Lambda_{5,6}$ | [111] | II-IV | +0.407(+0.240[f]) | -33(+13[f]) |
| | | | | I | -1.222 | + 3 |
| +0.205 | $A(Be,H)_1$ | $\Lambda_{5,6}$ | [111] | II-IV | +0.407(+0.517[f]) | +11(-13[f]) |
| | | | | I | -1.222 | - 4 |
| | $A(Be,H)_2$ | $\Lambda_4$ | [111] | I | +1.222 | g |
| | | | | II-IV | -0.407(-0.517[f]) | +28(+1[f]) |
| h | A(Zn,H) | $\Lambda_{5,6}$ | [111] | II-IV | +0.407 | +46 |
| | | | | I | -1.222 | +10 |

[a]Values given are the shifts of hole binding energy per unit compressional stress, $-\delta E/T$.

[b]The representations indicated are those of the acceptor states in the absence of applied stress.

[c]Deviation is expressed in terms of a percentage of the theoretical value.

[d]Although the deviation is not mathematically defined, agreement is excellent.

[e]No experimental data exist for comparison.

[f]These values are the result of a linear least-squares fit to the nonlinear theoretical expression (12), evaluated at the stress values experimentally used.

[g]Spectral interference precludes quantification of this shift; see text.

[h]This value cannot be determined because the second (1s)-like level has not yet been detected.

FIG. 1. PTI spectrum of a sample containing A(D,C), aluminum and a trace of boron.

FIG. 2. PTI spectra of the D and C transitions of aluminum, and the D transition of $A(D,C)_2$, under uniaxial compression along: (a) [111]; (b) [100]; (c) [110]. These spectra were recorded at 7.0 K.

FIG. 3. Energy shifts of the D transition of $A(D,C)_2$ under uniaxial compression along [111], [100] and [110]. The points $D_1,\ldots,D_4$ are the observed peak positions. The lines indicate the shifts of the ground-state levels. For [100], the final-state level splits into two levels, giving rise to the observed splitting $D_2 - D_1$. For [110], the splitting $D_2 - D_1 = D_4 - D_3$ arises from the final-state level.

FIG. 4. PTI spectra of the D transitions of $A(H,Si)_1$, $A(H,Si)_2$ and aluminum, under [111] uniaxial compression. In square brackets, the numbers "1" and "2" refer to $A(H,Si)_1$ and $A(H,Si)_2$, respectively.

FIG. 5. Energies of the D transitions of $A(H,Si)_1$ and $A(H,Si)_2$, under [111] uniaxial compression.

FIG. 6. PTI spectra of the D transitions of $A(Be,H)_1$, $A(Be,H)_2$, boron and aluminum, under [111] uniaxial compression. In square brackets, the numbers "1" and "2" refer to $A(Be,H)_1$ and $A(Be,H)_2$, respectively. These spectra were recorded at 6.0 K.

FIG. 7. The piezospectroscopic behavior of the two (1s)-like levels of differently oriented, trigonal shallow acceptor complexes, based on the model discussed here. (a) Trigonal distortion equivalent to a stress of +0.205 kbar (tensional); (b) Trigonal distortion equivalent to a stress of -0.810 kbar (compressional). Roman numerals denote the four possible orientations of the complexes. "$\Lambda_4$" and "$\Lambda_{5,6}$" denote the representations of $\overline{C}_{3v}$ according to which the states transform in the absence of externally applied stress. The energy shifts are shown for applied uniaxial compression; under tension, the behavior of (a) and (b) is reversed, as explained in the text.

FIG. 8. The piezospectroscopic behavior of the two (1s)-like levels of differently oriented, rhombic I shallow acceptor complexes, based on the model discussed here. In order to model the behavior of nearly tetragonal, rhombic I complexes, the <100> equivalent stress P is taken to be four times as large as the <110> equivalent stress Q. (a) Tensional equivalent stresses; (b) Compressional equivalent stresses. Roman numerals denote the six possible orientations of the complexes. "$\Delta_5$" denotes the representation of $\overline{C}_{2v}$ according to which the states transform in the absence of externally applied stress. In parenthesis, "$X_6$" and "$X_7$" denote the representations of $\overline{D}_{2d}$ according to which they would transform in the absence of applied stress, and when Q = 0. The energy shifts are shown for applied uniaxial compression; under tension, the behavior of (a) and (b) is reversed, as explained in the text.

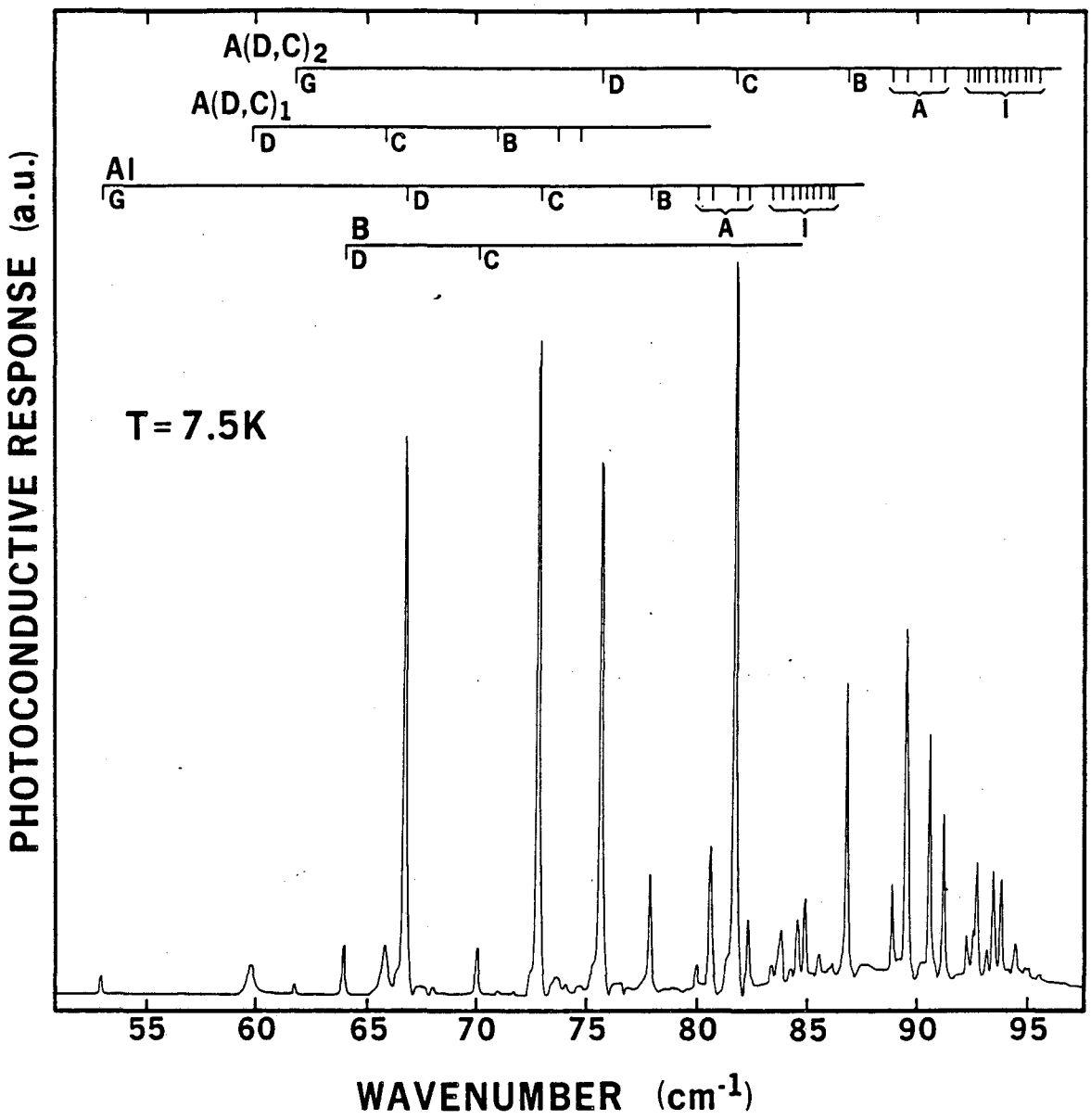


XBL 863-1160

Fig. 1.

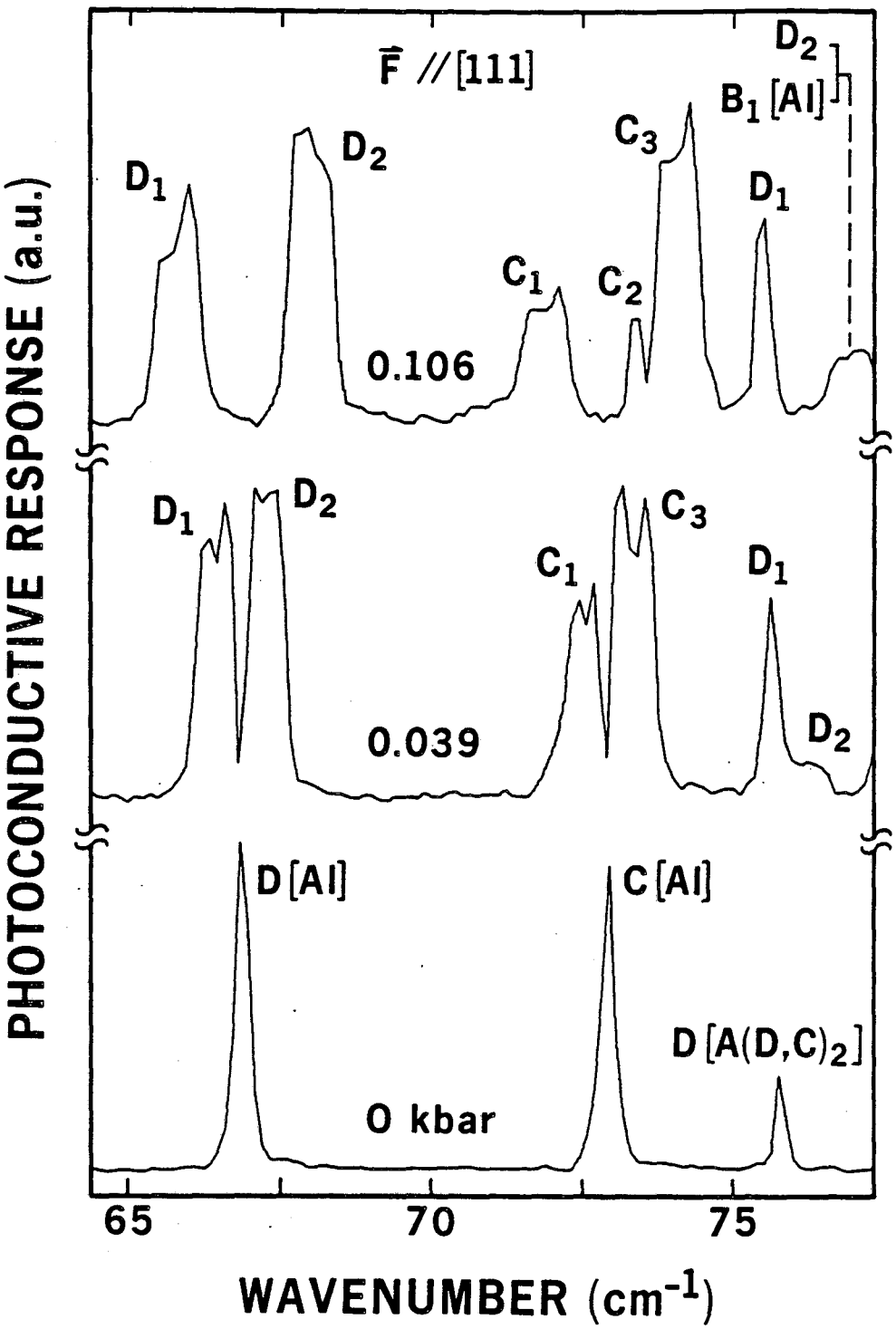


XBL 8611-4390

Fig. 2(a).

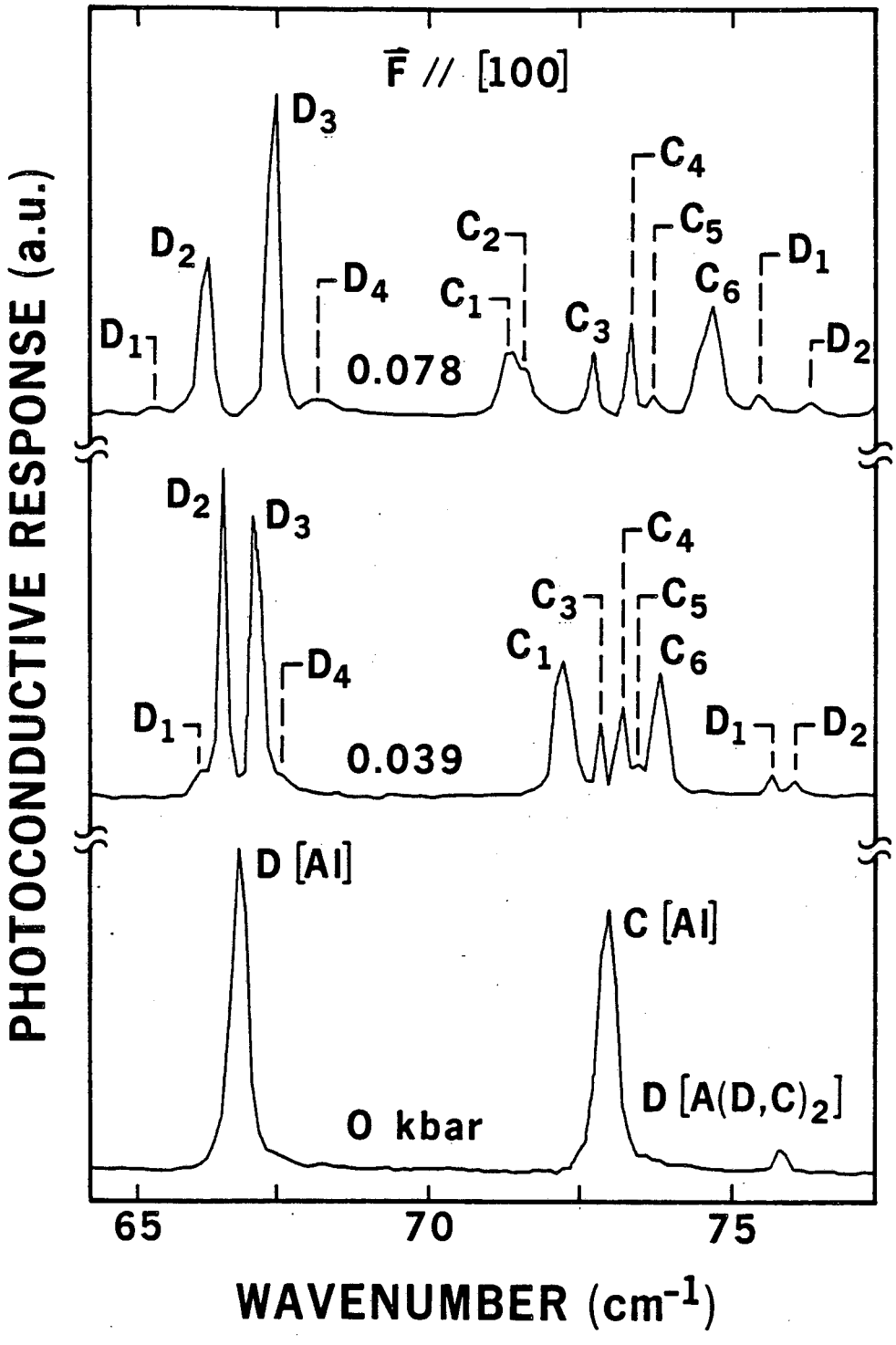


XBL 8611-4389

Fig. 2(b).

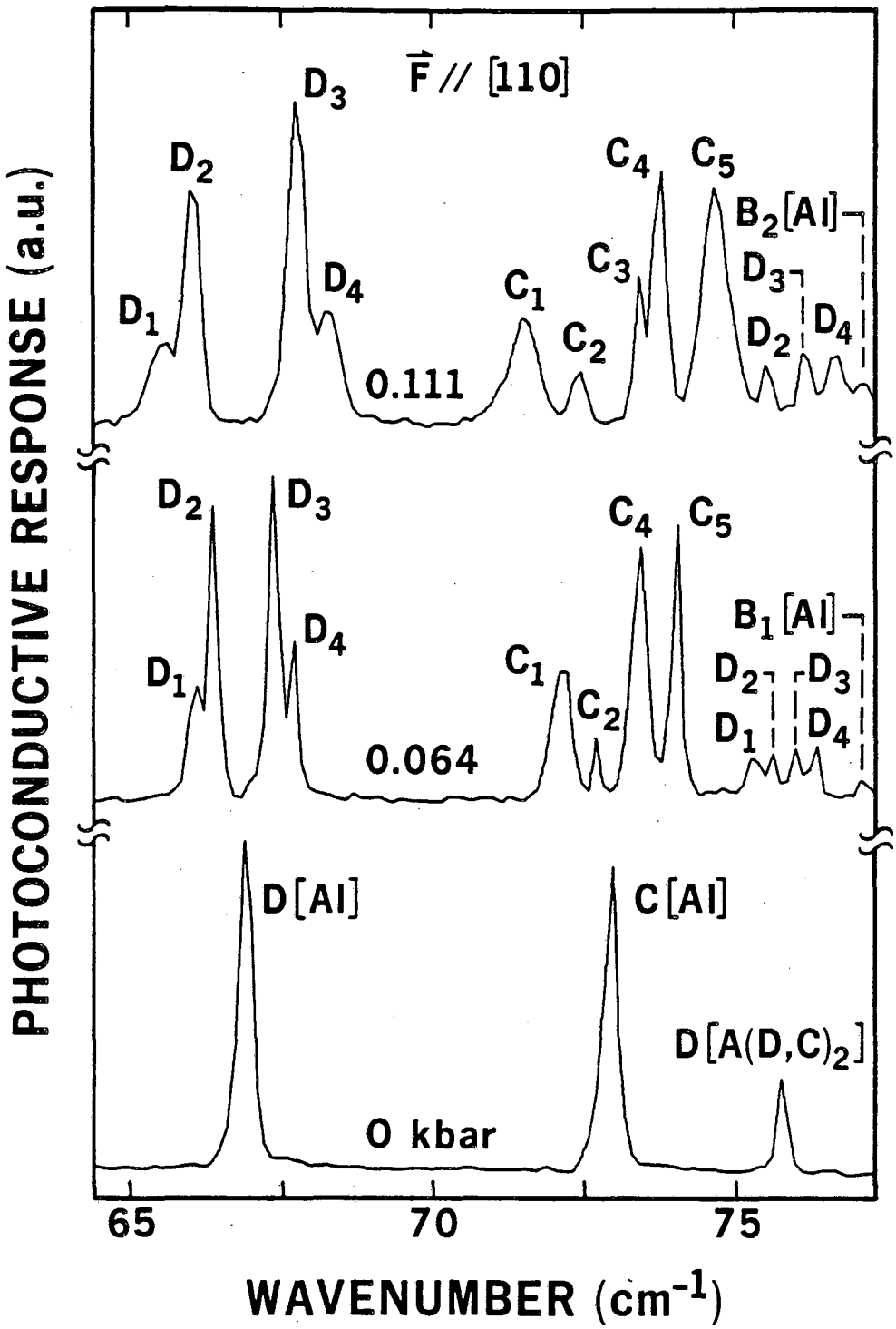


XBL 8611-4388

Fig. 2(c).

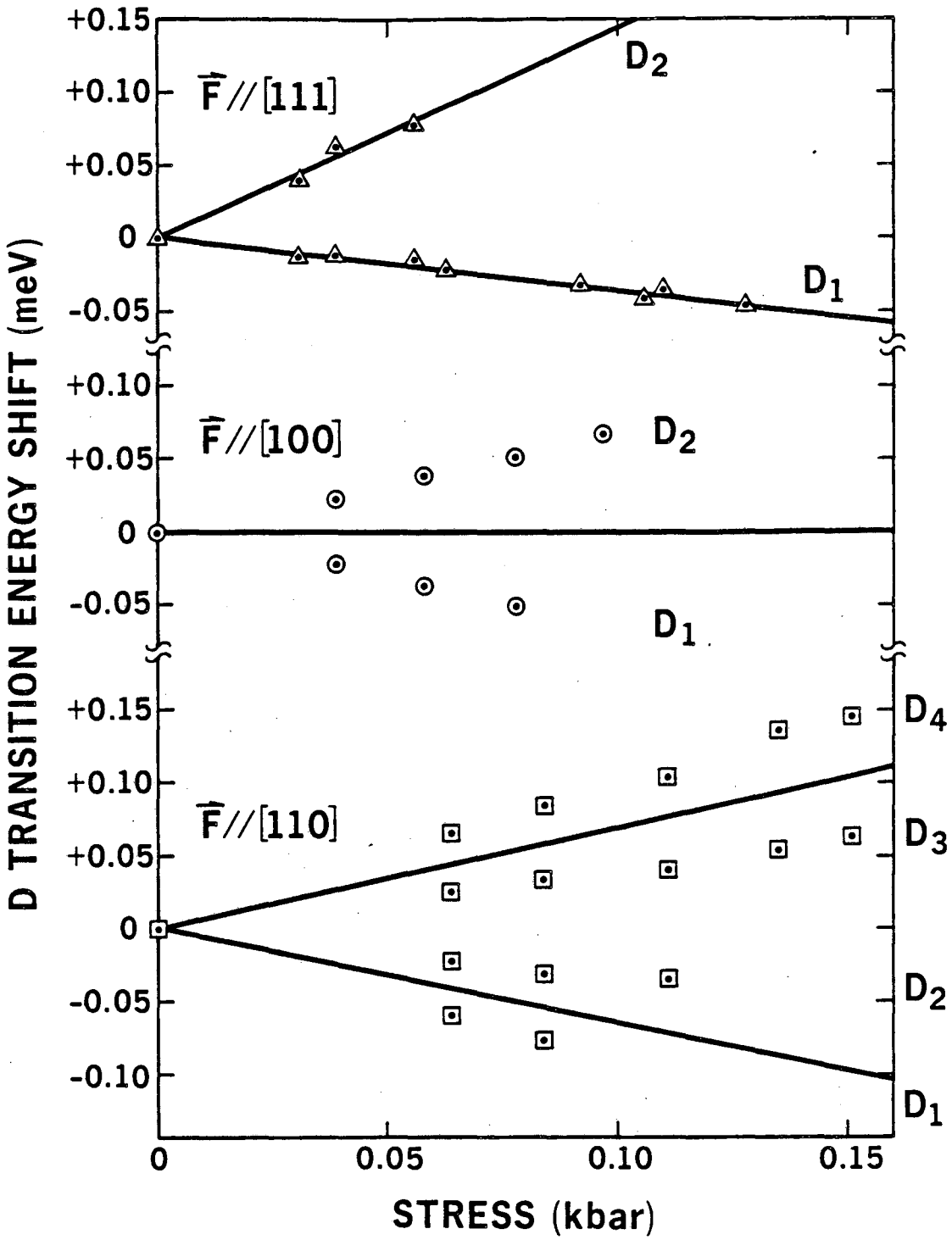


XBL 8611-4392

Fig. 3.

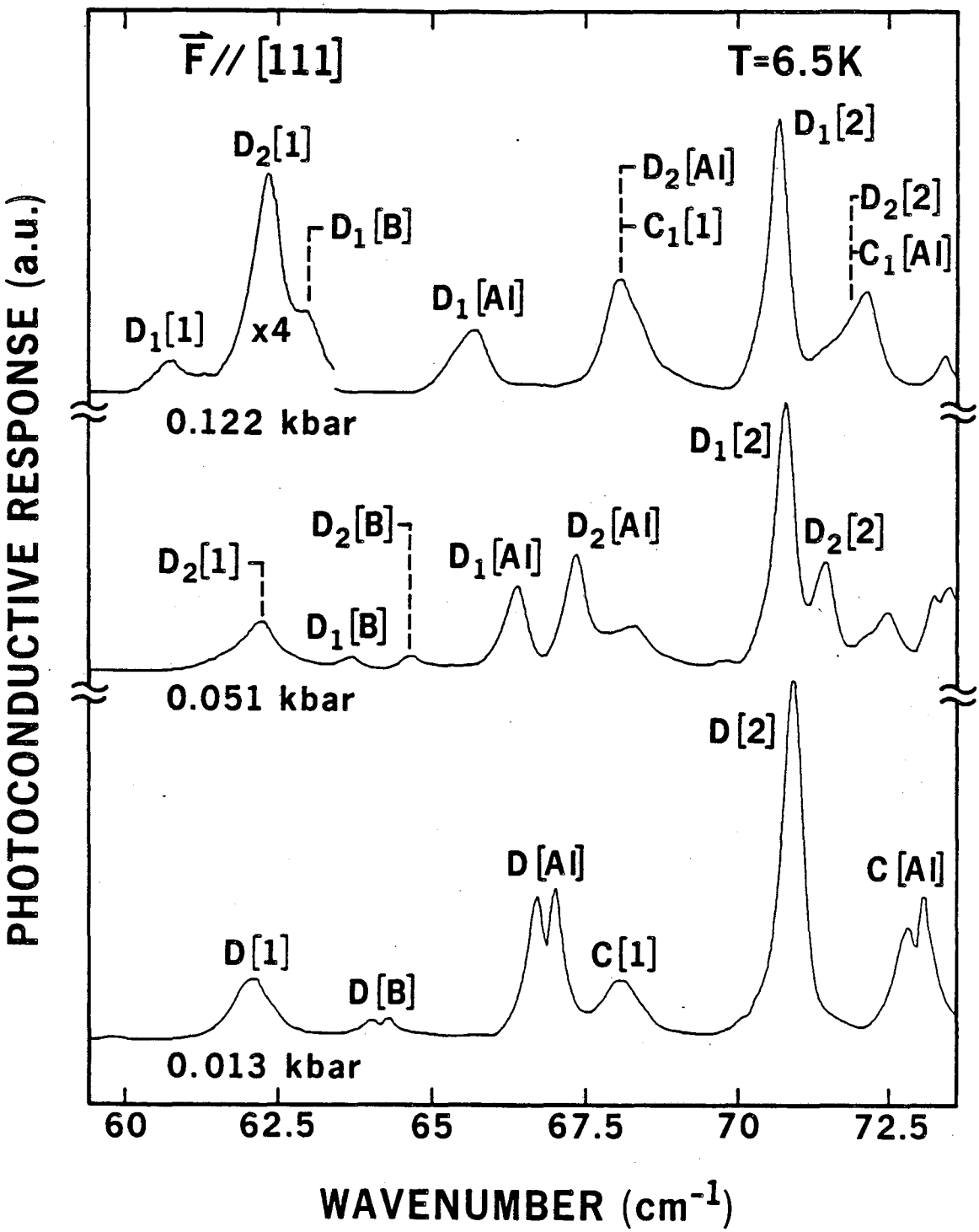


XBL 874-1719

Fig. 4.

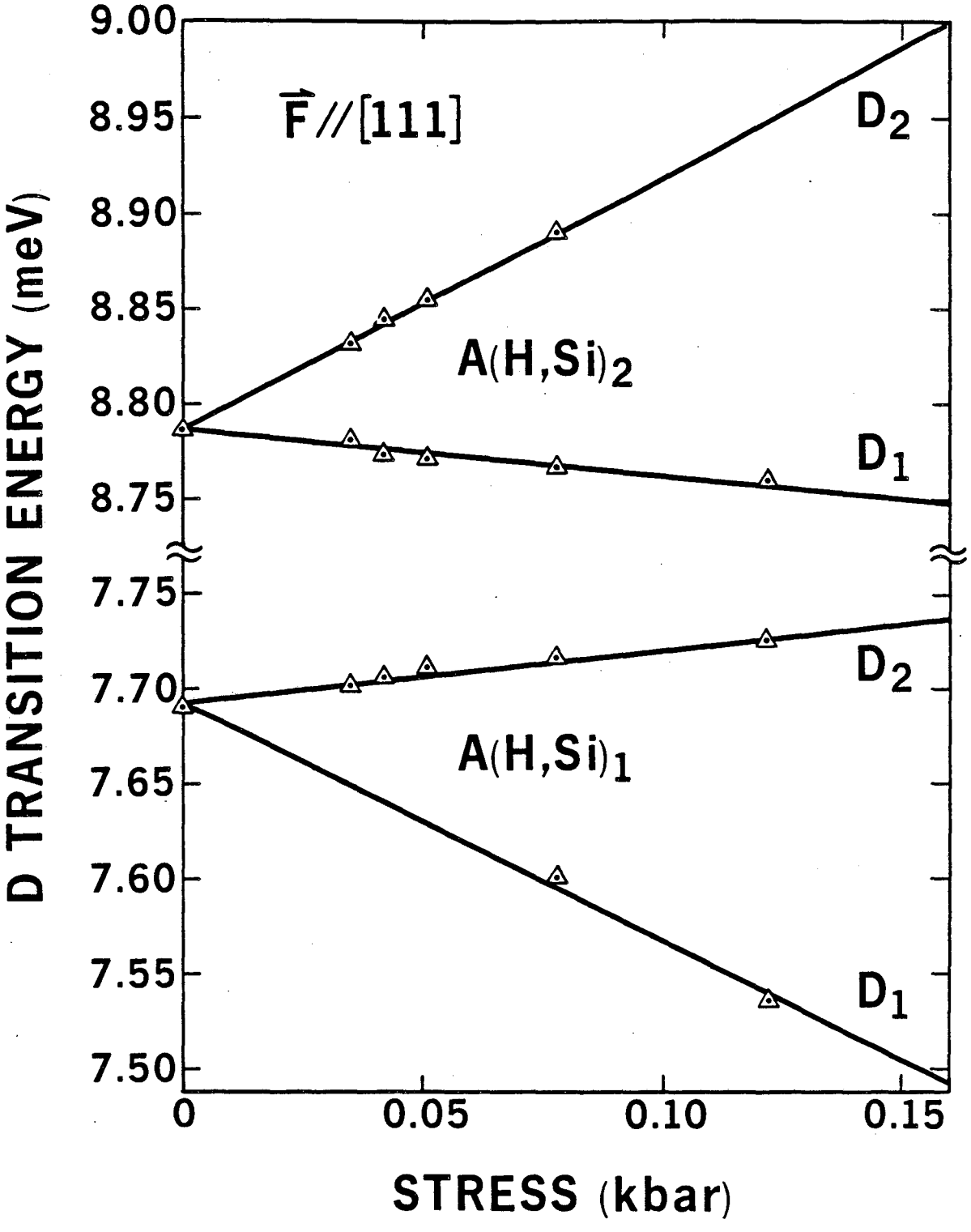


XBL 874-1720

Fig. 5.

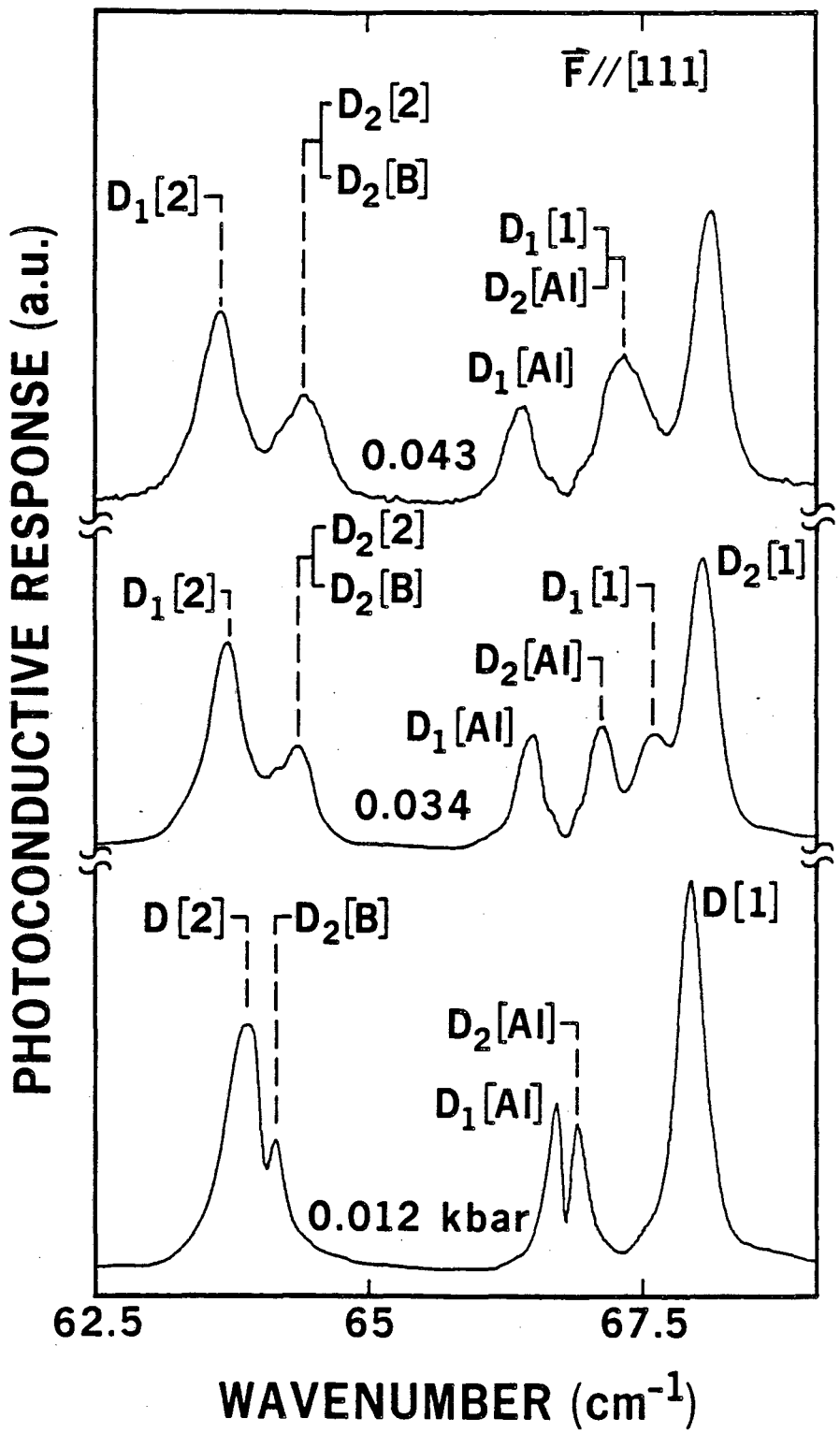


XBL 8611-4402

Fig. 6.

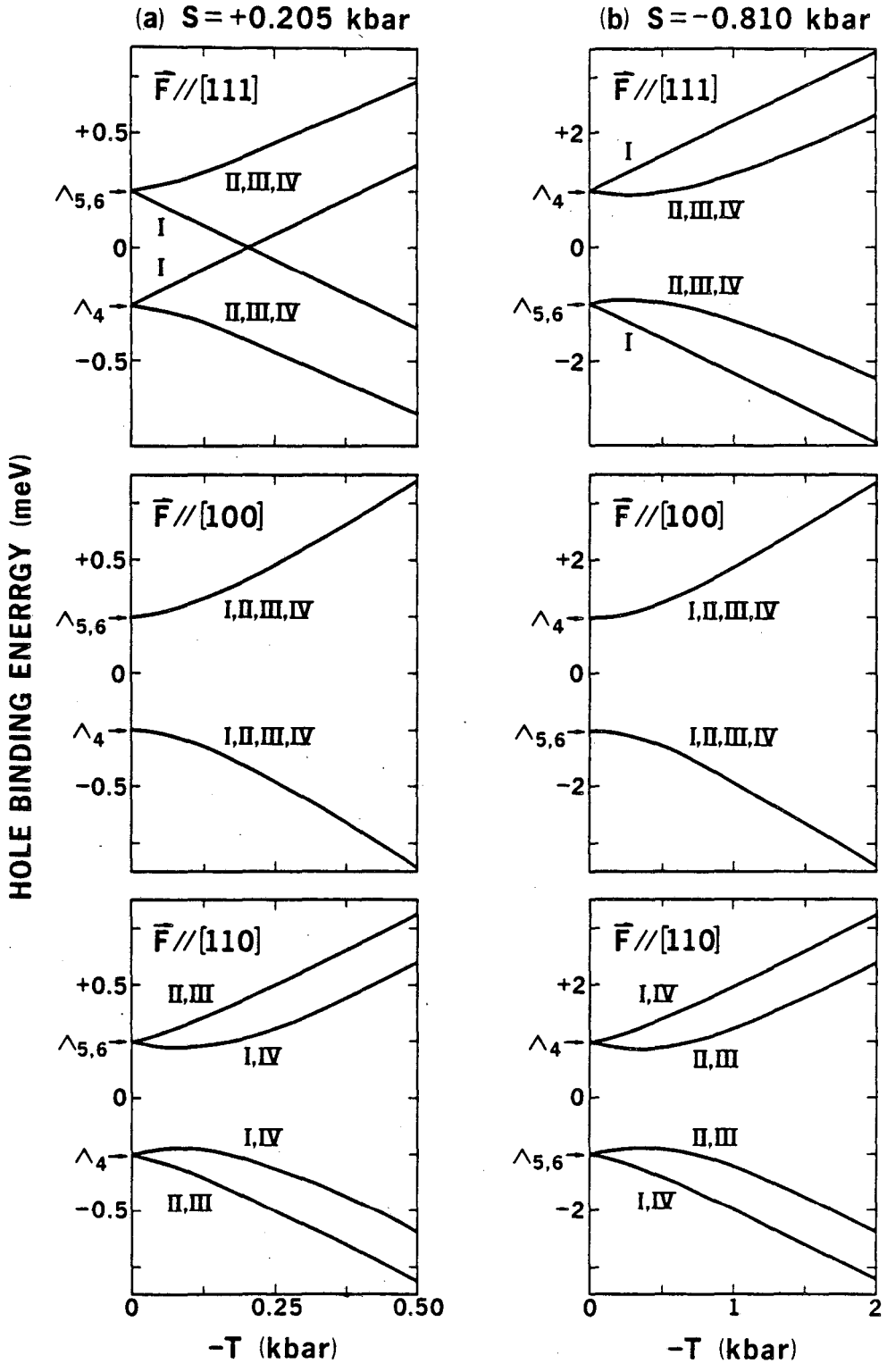
(a) S=+0.205 kbar
(b) S=-0.810 kbar
F//[111]
F//[100]
F//[110]
HOLE BINDING ENERGY (meV)
-T (kbar)
XBL 8611-4400

Fig. 7.

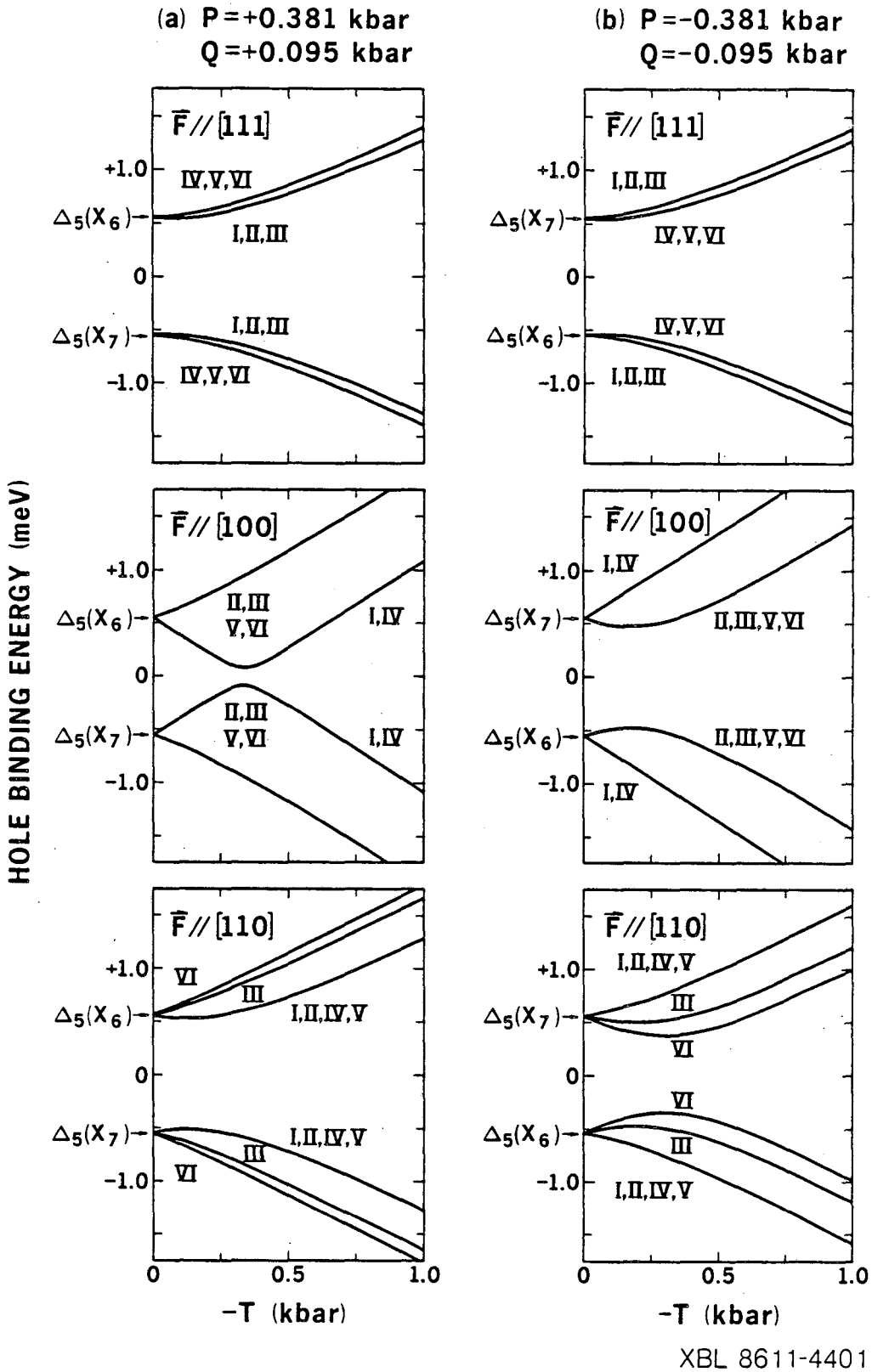


XBL 8611-4401

Fig. 8.

*LAWRENCE BERKELEY LABORATORY*
*TECHNICAL INFORMATION DEPARTMENT*
*UNIVERSITY OF CALIFORNIA*
*BERKELEY, CALIFORNIA 94720*